A Framework for Privacy Preserving Localized Graph Pattern Query Processing

ABSTRACT

This paper studies privacy preserving graph pattern query services in a cloud computing paradigm. In such a paradigm, data owner stores the large data graph to a powerful cloud hosted by a service provider (SP) and users send their queries to SP for query processing. However, as SP may not always be trusted, the sensitive information of users' queries, importantly, the query structures, should be protected. In this paper, we study how to outsource the *localized graph pattern queries* (*LGPQ*s) on the SP side with privacy preservation. *LGPQ*s include a rich set of semantics, such as *subgraph homomorphism*, *subgraph isomorphism*, and *strong simulation*, for which each matched graph pattern is located in a subgraph called *ball* that have a restriction on its size. To provide privacy preserving query service for *LGPQ*s, this paper proposes the first framework, called Prilo, that enables users to privately obtain the query results. To further optimize Prilo, we propose Prilo* that comprises the first bloom filter for trees in the trust execution environment (*TEE*) on SP, a query-oblivious twiglet-based technique for pruning non-answers, and a secure retrieval scheme of balls that enables user to obtain query results early. We conduct detailed experiments on real world datasets to show that Prilo* is on average 4x faster than the baseline, and meanwhile, preserves query privacy.

1 INTRODUCTION

Graph pattern queries have been proposed in the literature (*e.g.*, [13, 41, 50]), and used in many recent applications, such as social network analysis, biology analysis, electronic circuit design, and chemical compound search [43, 48, 49, 59, 64]. On one hand, graph patterns often have high computational complexities. On the other hand, different from matching the query to the whole data graph (*e.g.*, graph simulation [41]), graph pattern results that span through small subgraphs can be preferred, *e.g.*, in applications where humans would interpret the results. Hence, *localized graph pattern queries* (*LGPQ*), such as *subgraph homomorphism query* (*hom*) [30], *subgraph isomorphism query* (*sub-iso*) [13], and *strong simulation query* (*ssim*) [40], whose semantics require a size restriction on the matched patterns, have recently received much attention, *e.g.*, [19, 25, 47, 57].

As *data owner*s and *query user*s may not always have the IT infrastructure to processing *LGPQ*s on the graph data, database outsourcing (such as to a *service provider* (SP) equipped with a cloud) has advantages to both of them, including elasticity, high availability, and cost savings. Database outsourcing inevitably has data privacy concerns. In particular, in the semi-honest model, the SP may infer sensitive information from both the queries and their processing. In Example 1, we illustrate the efficiency and query privacy challenges of this problem.

SIGMOD '2023, June 18–23, 2023, Seattle, WA

ACM ISBN 978-1-4503-XXXX-X/18/06…$15.00
https://doi.org/XXXXXXX.XXXXXXX

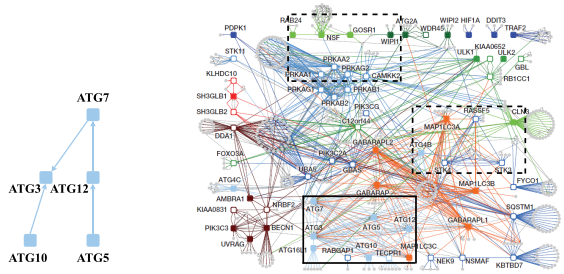

(a) An autophagy pattern **(b) A *PPI* Network for Human Autophagy**[1]

Figure 1: Example of outsourcing *LGPQ* for biology analysis

EXAMPLE 1. *Consider a biotechnology company whose competitive advantages are its biological discoveries. The company has recently found a potentially valuable autophagy pattern, as shown in Fig. 1(a). To explore the autophagy patterns with the same or similar structures as the found one, it therefore uses an* LGPQ *to retrieve the subgraph data from an* SP*, who has a powerful IT infrastructure to host a publicly known large protein-protein interaction (*PPI*) network for autophagy interaction in human cells, as shown in Fig. 1(b). It may evaluate an* LGPQ *on small subgraphs, e.g., the solid box in Fig. 1(b). However, it neither evaluates the query on* all *the possible subgraphs (e.g., the dotted boxes in Fig. 1(b)) nor exposes the autophagy pattern (i.e., the query structure) to the* SP *side. Similar scenarios on other graphs, e.g., collaboration networks and social networks, can also be found [18, 39, 57].* □

Existing works [18, 57] consider privacy preserving *LGPQ* under *individual* semantic, in particular, *sub-iso* queries [18] and *ssim* queries [57], and propose optimizations that focus on either minimizing the size of candidates to be matched or reducing the false positives of query results. Moreover, almost all existing works determine only the *existence* of matches in the data graphs. Except a trivial baseline [57], no previous work retrieves query matches as query results. In this paper, we take the first step towards the *first general* framework for finding the matches of *LGPQ*s with an SP. However, there are two main challenges.

Challenge 1: To design general privacy preserving steps for LGPQ*s.*

To address this challenge, we propose a privacy preserving framework, called Prilo, that comprises three general steps, namely, *candidate enumeration*, *query verification*, and *query matching*. The privacy preserving computation in these steps is done one ball at a time [40], where a ball is a subgraph of the graph defined by its center and radius, as the units (supersets) of *LGPQ* results. Since a ball can be much smaller than the whole graph, its privacy preserving processing can be efficient. The balls can also be precomputed, encrypted, and stored on the SP side.

To implement the privacy preserving processing on SP, we need to strike a balance between the efficiency and security of cryptography tools used. In particular, it has been known that fully homomorphic

[1] C. Behrends, M. E. Sowa, S. P. Gygi, and J. W. Harper. Network organization of the human autophagy system. Nature, 466(7302):68, 2010.

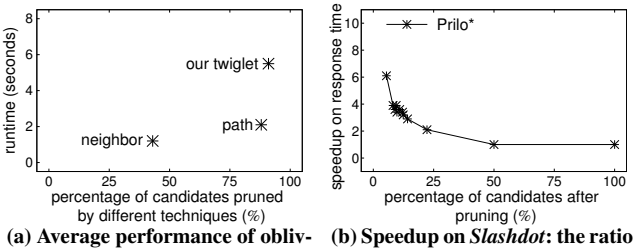

(a) Average performance of oblivious pruning by using different topologies: 3-hop neighbor's label [17], paths [57] and our twiglets of 4 labels from experiments

(b) Speedup on *Slashdot*: the ratio of Prilo*'s runtime (the time for user to obtain first query results from SP) to the runtime without Prilo*'s optimizations

Figure 2: Some highlights of performance of Prilo*

encryptions (*FHE*) [20] and some partial homomorphic encryptions (*PHE*s), *e.g.*, *Paillier* [44], can be inefficient. We adopt an efficient symmetric encryption scheme called *cyclic group based encryption* (*CGBE*) [17] that is *CPA*-secure. In particular, to implement query verification, we use *CGBE* in a *query-oblivious* manner to detect the violations of the *LGPQ* semantics on the balls. Users then retrieve from SP the balls that have no violations. Users decrypt such balls, and compute query matches using existing algorithms on plaintext.

Challenge 2: To propose privacy preserving optimizations for Prilo.

It is evident that there can be *spurious balls* on SP, *i.e.*, balls that contain *no matches or duplicated matches*, and they should be *"pruned"*, *i.e.*, users *skip evaluating queries on them*. Hence, we propose Prilo* to optimize Prilo. In a nutshell, SP computes *pruning messages* to indicate whether balls are spurious or not, and users decrypt them to recognize non-spurious balls and skip spurious ones.

More specifically, the first technique in Prilo* is to exploit the *trusted execution environment* (*TEE*), *e.g.*, the *Intel software guard extensions* (SGX) [14]. Despite its popularity for ensuring its application's security, to our knowledge, it has not been exploited in privacy preserving *LGPQ*s. We propose to enumerate some small tree structures of the query by users for pruning inside the enclave of SGX. It is known that SGX's enclave has a limited memory space. Hence, we propose to use bloom filters inside the enclave to compute pruning messages. The second technique is to propose a small structure called *twiglet* for query-oblivious pruning under the ciphertext domain, without the need of *TEE*. While previous work proposed simpler topologies for query-oblivious pruning, as shown in Fig. 2(a), twiglet can further enhance computing pruning messages at the expense of an additional runtime. To balance the pruning power and runtime, users can tune the size of twiglets.

The third technique optimizes the retrieval of non-spurious balls. We propose two kinds of SP servers (called Players and Dealer), and importantly, they enable that the non-spurious balls are securely returned to users early, while some dummy balls are also returned to make the ball retrieval patterns query-oblivious to SP. Then, users can compute all the matches early, as opposed to waiting the SP to finish its computation. From our preliminary experiments, we observe that on average, only 15% candidate balls contain matches. Specifically, on the SP side, a special server called Dealer uses pruning messages to generate sequences of balls mixed with dummy balls where non-spurious balls are placed in the front, in a secure way. The other servers called Players conduct *LGPQ* evaluation according to the sequences, without the knowledge of the balls' pruning messages. These together result in the servers sending to users the balls that contain matches early, while query's privacy is preserved from SP. By using these optimization ideas, Prilo* can achieve a 4x speedup on *Slashdot* for the runtime for the users to obtain the first match pattern (Fig. 2(b)).

Contributions. The contributions of this paper are as follows.

- We propose the first *secure* general framework for *LGPQ*, called Prilo. Prilo has a unified encoding to encrypt the queries online. Prilo comprises three general steps for processing *LGPQ*, namely candidate enumeration, query verification, and query matching.
- We propose an optimized framework called Prilo* that comprises i) a *bloom filter* checking that is the first to exploit *TEE* for pruning for *LGPQ*, ii) twiglets for a query-oblivious pruning, which does not need *TEE*, and iii) the first secure retrieval scheme that uses two kinds of servers in SP to return the evaluated results of non-spurious balls to users early for computing matched patterns, while existing works only check their existence.
- We present the results of the privacy analyses and their proof sketches on Prilo*. The detailed proofs are presented in [2].
- Our experiments verify that Prilo*'s pruning techniques outperform the SOTA on the pruning power with similar time cost and the query results are returned earlier than the baseline, in particular, 4x, 5x, and 8x faster than the baseline on *Slashdot*, *DBLP*, and *Twitter*, respectively. Our experiment with *LDBC* shows that Prilo is efficient for most of the queries and Prilo* furthers optimizes Prilo in 5 out of 10 queries, while Prilo and Prilo* exhibit similar performance in the other 5 queries.

Organization. The preliminaries and the problem statement are presented in Sec. 2. Sec. 3 presents the Prilo framework. Prilo*'s optimizations, the pruning techniques together with a secure scheme for ball retrieval, are presented in Sec. 4. Sec. 5 reports the privacy analysis. Sec. 6 reports the experimental results and Sec. 7 discusses the related work. This paper is concluded in Sec. 8.

2 PRELIMINARIES AND BACKGROUND

2.1 Notations of Graphs and Queries

This subsection presents some notations for describing *LGPQ*.

Graph. A *graph* is denoted by $G = (V_G, E_G, \Sigma_G, L_G)$, where V_G, E_G, Σ_G, and L_G are the sets of vertices, directed edges, and labels, and the function for matching a vertex to its label, respectively. (u, v) denotes the directed edge from u to v, where $u, v \in V_G$, and $L_G(u)$ denotes the label of u. For graph G, the *distance* between u and v in G, denoted by $\text{dis}(u, v)$, is the length of the shortest undirected paths from u to v in G [40], and the *diameter* of G, denoted by d_G, is the largest distance between any pairs of vertices of G.

Ball [40]. A *ball*, denoted by $G[u, r]$, is a connected subgraph $B = (V_B, E_B, \Sigma_B, L_G, u, r)$ of graph G which takes u in G as *center*, and r as the *radius*, s.t. i) $V_B = \{v | v \in V_G, \text{dis}(u, v) \leq r\}$, ii) E_B has the edges that appear in G over the same vertices in V_B, and iii) $\Sigma_B = \{L_G(v) | v \in V_B\}$.

Adjacency matrix. The *adjacency matrix* of graph G, denoted by M_G, is a $|V_G| \times |V_G|$ matrix. Given vertex u (*resp.* vertex v) that locates in the i^{th} row (*resp.* the j^{th} column) of a matrix M, $M(i, j)$ is also denoted by $M(u, v)$ for simplicity. Then, $M_G(i, j) = 1$ if $(u, v) \in E_G$. Otherwise, $M_G(i, j) = 0$. The i^{th} row vector of a matrix M is

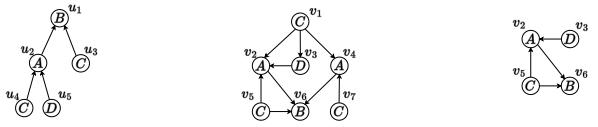

Figure 3: An example for a *hom* subgraph in G of Q

denoted by $M(i)$. We may omit the subscript, such as G, when it is clear from the context.

Some popular query semantics of localized graph pattern queries, namely, *subgraph homomorphism* (*hom*), *subgraph isomorphism* (*sub-iso*), and *strong simulation* (*ssim*), can be readily expressed by using *matrices* [17, 57]. We illustrate this with *hom* as follows.

DEFINITION 1. *(**Subgraph homomorphism** (**hom**)) Given a connected query Q and a graph G, a* subgraph homomorphism *of Q in G is a match function $\mathcal{H}$: $V_Q \rightarrow V_G$ that satisfies the following conditions.*

(1) $\forall u \in V_Q$, $L_Q(u) = L_G(\mathcal{H}(u))$; and

(2) $\forall u, v \in Q$, $M_Q(u, v) = 1 \Rightarrow M_G(\mathcal{H}(u), \mathcal{H}(v)) = 1$. □

Sub-iso can be defined by modifying the match function $\mathcal{H}$ of Def. 1 with an injective function [17].[2] Due to space restrictions, we present the definition of *ssim* [57] in App. A.1 of the technical report [2]. Given a query semantic $\mathcal{F}$ (*e.g.*, *hom*, *sub-iso*, or *ssim*) and the vertex set $\{\mathcal{H}(v)|v \in V_Q\}$, an induced subgraph of the set in graph G is called a *matching subgraph* for Q under $\mathcal{F}$.

EXAMPLE 2. *Consider the query Q and the graph G in Fig. 3. The induced subgraph of $\{v_2, v_3, v_5, v_6\}$ at the RHS of Fig. 3 is a matching subgraph of G for Q under* hom*, where $\mathcal{H}(u_1) = v_6$, $\mathcal{H}(u_2) = v_2$, $\mathcal{H}(u_3) = v_5$, $\mathcal{H}(u_4) = v_5$, and $\mathcal{H}(u_5) = v_3$.*

It is evident from Def. 1 and Example 2 that each matching subgraph for a *hom* query exists in a ball with a radius equal to d_Q. We are ready to give the definition of the query studied in the paper.

Localized graph pattern query (*LGPQ*). Given a query semantic $\mathcal{F}$, a *localized graph pattern query* $Q = (V_Q, E_Q, \Sigma_Q, L_Q, \mathcal{F})$ on a graph G is to find matching subgraphs for Q under $\mathcal{F}$ for each ball $G[u, d_Q]$, where $u \in V_G$ and $\mathcal{F} \in \{hom, sub\text{-}iso, ssim\}$.

2.2 Background on Cryptosystem and Trusted Execution Environment

The security tools used in the technical presentation are as follows.

Cyclic group based encryption (CGBE) **[17].** CGBE is a *CPA-secure* symmetric encryption scheme that supports the following homomorphic operations.

$$D(E(m_1) + E(m_2)) = m_1 \cdot r_1 + m_2 \cdot r_2$$
$$D(E(m_1) \cdot E(m_2)) = m_1 \cdot m_2 \cdot r_1 \cdot r_2,$$

where i) m_1, $m_2 \in \mathbb{Z}_p$, ii) r_1 and r_2 are two random numbers, and iii) $E(m)$ and $D(m)$ denote the encryption and decryption of message m, respectively. CGBE's homomorphic operations will be used to design the privacy preserving solution by computation of encrypted messages. Note that CGBE requires $m_1 + m_2$ and $m_1 \cdot m_2$ are smaller than a large public prime p, or there are overflow errors [57].

[2] In some existing works [30, 32], the match function $\mathcal{H}$ of *hom* (or *sub-iso*) also requires that the labels of the edges (u, v) and $(\mathcal{H}(u), \mathcal{H}(v))$ are the same. For simplicity, we omit this requirement since it can be efficiently handled by transforming each edge (u, v) into an intermediate vertex with (u, v)'s edge label.

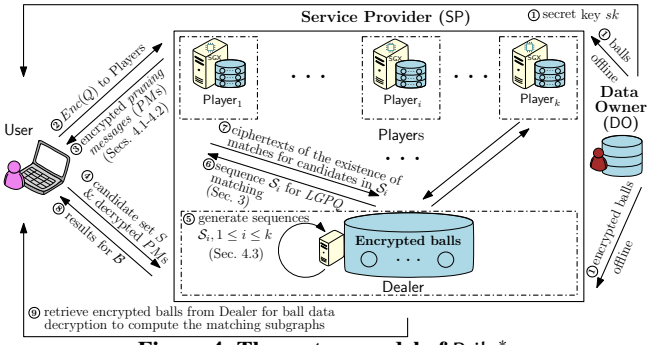

Figure 4: The system model of Prilo*

Trusted execution environment (*TEE*). Secure co-processors have recently been found efficient and effective in building secure applications. In particular, modern *Intel* CPUs have supported the software guard extensions (SGX) [14], a set of x86 instruction set architecture extensions, to construct a *TEE*. SGX provides users a secure and isolated hardware container called *enclave*. A secure channel is established between users and the enclave. A user encrypts the query and sends the encrypted query into the enclave for secure computation. The secure memory region in SGX is approximately 128 MB [3, 4, 56]. However, the cost of interaction with the enclave is huge that it is desirable to design space-efficient techniques when applying SGX for secure computation.

2.3 Models and Problem Statement

This subsection presents the background of the system model and security model, and then presents our problem statement.

System model. We extend the commonly used system model on outsourced databases [15, 33, 55] that includes *data owner*, *user*, and *service provider*. Fig. 4 shows an overview of our system model.

- **Data owner** (DO). A data owner first generates a secret key sk and all balls of graph G with various diameters offline. For each ball B of G, data owner ① uses sk to encrypt B before sending B or the encrypted B to two different kinds of cloud servers on the service provider, respectively. Only authorized users can obtain sk.
- **User**. User ② sends to the service provider a query encrypted by using the private key pk of CGBE. After ③ receiving the encrypted *pruning messages* (*PM*s) of candidate balls, User decrypts these *PM*s, and then ④ sends the decrypted *PM*s and ball identifier set S of candidate balls to the service provider. After ⑧ receiving the ciphertext results about whether there exist matching subgraphs in candidate balls, User decrypts these results to find the target ball identifiers and then ⑨ retrieves the encrypted target balls from the service provider. Finally, User decrypts the encrypted balls with sk and computes the matching subgraphs for the query.
- **Service provider** (SP). We extend the SP of the widely used system model [15, 33, 55], to allow some optimizations enabled by SGX and to facilitate secure ball retrieval. Assume that SP consists of two kinds of servers, namely k ($k \ge 2$) *player server*s (Players) equipped with SGX and a *dealer server* (Dealer), for ball retrieval. After ② receiving the encrypted query from User, the Players compute for each candidate ball B, under the ciphertext domain or inside SGX's enclave, the PM that indicates whether B may contain a match (a.k.a matching subgraph) of the query. Then, Players ③ send the PMs

of candidate balls to User. After ④ receiving the set S of candidate ball's identifiers and their decrypted PMs from User, Dealer ⑤ generates a sequence $\mathcal{S}_i$ of ball identifiers based on the set S and PMs, and ⑥ sends $\mathcal{S}_i$ to Player$_i$, $1 \le i \le k$. For balls in $\mathcal{S}_i$, Player$_i$ run secure matching algorithms to generate a ciphertext result that indicates the existence of matching subgraphs. Player$_i$ ⑦ sends the ciphertext results of balls in $\mathcal{S}_i$ back to Dealer and then, Dealer ⑧ sends the ciphertext results of balls of S to User.

Security model. This paper assumes the SP is honest but curious, *a.k.a.* the *semi-honest adversary model* that is widely adopted in the literature [10, 11, 24, 36]. In a nutshell, SP performs the agreed computation protocol but may infer the private information. We made a mild assumption on SP. As shown in Fig. 4, there are multiple Players and a Dealer on SP. Unlike the existing multi-party computation (*MPC*) [6] where the servers communicate with others, Players only communicate with Dealer and Players do not collude with each other, which is similar to a recent work [35]. Regarding the communications between Players and Dealer, we adopt the commonly used collude-resistant model [15, 29, 37, 38] that Dealer and Players do not collude. We also assume the servers on SP adopt the *chosen plaintext attack* (*CPA*) [36], *i.e.*, the adversaries can choose arbitrary plaintexts to obtain their ciphertexts to gain sensitive information. The *privacy targets* of this paper are as follows.

- **Query privacy.** The structural information of User's query Q, *i.e.*, the value of each element in Q's adjacency matrix.
- **Access pattern privacy.** When querying on a graph, the access pattern privacy requires that the access pattern and the values of involved data during the computation process have no relations to the query privacy. That is, the computation process is *query-oblivious*.

Problem statement. *Assume the system and security models presented in Sec 2.3. Given an* LGPQ $Q = (V_Q, E_Q, \Sigma_Q, L_Q, \mathcal{F})$ *and a graph G, the goal is to compute all the subgraphs of G that can be matched to Q under $\mathcal{F}$ when preserving the privacy target.*

3 THE Prilo FRAMEWORK

In this section, we propose a general framework called Prilo for handling *LGPQ*s. Fig. 5 shows the overview of Prilo. An *LGPQ* can be answered by three generic steps, namely *candidate enumeration*, *query verification*, and *query matching*. In the following subsections, we elaborate these steps with the query semantic of *hom*, as an example.[3] For simplicity, we may use *ball* to refer to *candidate ball*, when it is clear from the context.

3.1 Candidate Enumeration

In this subsection, we present how the candidate enumeration step enumerates all candidate subgraphs of a ball in a query-oblivious manner. We first propose two propositions to filter redundant balls.

PROPOSITION 1. *Given a query Q with diameter d_Q and label l ($l \in \Sigma_Q$), for any subgraph G_s of graph G, if G_s is a matching subgraph for Q under* hom*, there exists a vertex v in G such that i) $L_G(v) = l$, ii) G_s is a subgraph of $G[v, d_Q]$, and iii) $v \in G_s$.*

By Prop. 1, candidate enumeration can choose arbitrarily a label l from Σ_Q and consider as candidate balls *only* those balls having centers of label l and diameters equal to d_Q instead of all balls (① of Fig. 5). Then, we further derive Prop. 2.

Algorithm 1: Candidate Enumeration Algorithm (*hom*)

Input : A query Q with V_Q, Σ_Q, L_Q and d_Q, and a ball $B = G[w, d_Q]$
Output : The set R_1 of CMMs of all B's candidate subgraphs

Procedure `CanEnum(`V_Q, w, B, i, C, CV`)`:
1 **if** $i = 0$ **then**
2 $C \leftarrow 0$;
3 $(Q, B) \leftarrow$ `opt(`Q, B`);` `//opt():optimizations in [18]`
4 **foreach** $u \in V_Q$ **do**
5 $CV(u) \leftarrow \emptyset$; `//`$CV(u)$`:`$B$`'s vertices having label` $L_Q(u)$
6 **foreach** $v \in V_B$ **do**
7 **foreach** $u \in V_Q$ **do**
8 **if** $L_Q(u) = L_B(v)$ **then**
9 $CV(u) \leftarrow CV(u) \cup \{v\}$;
10 **if** $i = |V_Q|$ **then**
11 **if** $\forall u \in V_Q, C(u, w) = 0$ **then**
12 **return** $\emptyset$; `//`w `cannot be matched to any vertices of` Q
13 **return** $\{C\}$; `//`C `is a CMM`
14 $R_1 \leftarrow \emptyset$;
15 $u \leftarrow$ the $(i+1)^{\text{th}}$ vertex in V_Q;
16 **foreach** $v \in CV(u)$ **do**
17 $C(u, v) \leftarrow 1$; `//assign one 1 in the` $(i+1)^{\text{th}}$ `row`
18 $R_1 \leftarrow R_1 \cup$ `CanEnum(`Q, w, B, $i+1$, C, CV`)`;
19 $C(u, v) \leftarrow 0$;
20 **return** R_1;

PROPOSITION 2. *Given a query Q, a label l ($l \in \Sigma_Q$), and a ball $B = G[w, d_Q]$ of graph G, if there exists a subgraph B_s of B that B_s is a matching subgraph for Q under* hom *but $w \notin V_{B_s}$, there must exist a ball $B' = G[w', d_Q]$ of G that i) B_s is a subgraph of B', ii) $w' \in V_{B_s}$, and iii) $L_G(w') = l$.*

Props. 1 and 2 is established by a simple proof by following the definition of the ball and the *LGPQ* semantic. The proofs are presented in App. A.2 of [2]. With Props. 1-2, we can enumerate for a ball B only the *candidate subgraphs* that contains B's center. Moreover, if B's center cannot be matched to any vertices of the query, B can be considered as a *spurious* ball. Even if there can be a matching subgraph of B that does not contain B's center, it can be found from other balls. We remark that Props. 1-2 can be also applied to *sub-iso* and *ssim*.

To illustrate the enumeration of all candidate subgraphs of B for Q (*e.g.*, a *hom* query), we introduce the *candidate mapping matrix* to represent the match function $\mathcal{H}$ that matches V_Q to V_{B_c}, where B_c is a candidate subgraph of B.

DEFINITION 2. ***(Candidate mapping matrix (CMM))*** *A candidate mapping matrix from a query Q to a graph G, denoted by C, is a $|V_Q| \times |V_G|$ matrix that $\forall\, u \in V_Q$, $\exists\, v \in V_G$ satisfies i) $C(u, v) = 1$, ii) $L_Q(u) = L_G(v)$, and iii) $\forall\, w \in V_G - \{v\}$, $C(u, w) = 0$.*

EXAMPLE 3. *Consider the query Q and graph G in Fig. 3 and the match function $\mathcal{H}$ in Example 2. We locate vertex u_i, $1 \le i \le 5$ (resp. v_j, $1 \le j \le 7$) of Q (resp. G) on the i^{th} row (resp. the j^{th} column) of the* CMM*. Then, $\mathcal{H}$ can be represented by the* CMM *C that $C(u_1) = (0, 0, 0, 0, 0, 1, 0)$, $C(u_2) = (0, 1, 0, 0, 0, 0, 0)$, $C(u_3) = (0, 0, 0, 0, 1, 0, 0)$, $C(u_4) = (0, 0, 0, 0, 1, 0, 0)$, and $C(u_5) = (0, 0, 1, 0, 0, 0, 0)$, where $C(u_i, u_j) = 1$ represents matching u_i to v_j.*

Then, we present the algorithm to enumerate all CMMs of candidate subgraphs. Taking a query Q with V_Q, Σ_Q, L_Q and the diameter d_Q, and a ball B with the center w and radius d_Q as inputs, Alg. 1 returns the set R_1 of CMMs of all B's candidate subgraphs for *hom* queries as output. In Line 2, CMM C is initialized as a zero matrix.

[3] We remark that some *LGPQ* semantics may not require all three steps. *Sub-iso* can be extended with minor modifications on Sec. 3.1. *Ssim* is a special case that has a straightforward candidate enumeration step [40].

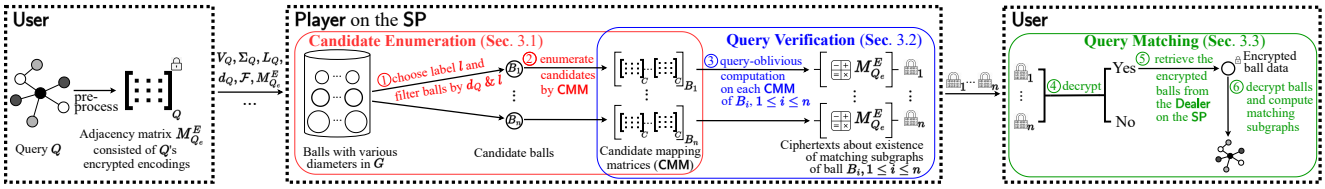

Figure 5: Overview of the Prilo framework

The optimizations [18] for minimizing the size of query Q (*resp.* ball B) on User (*resp.* Player) are applied in Line 3. $\forall u \in V_Q$, Lines 6-9 generate a vertex set $CV(u)$ that contains the vertices of B having the same label as u's label by comparing $L(u)$ with $L(v)$, $v \in V_B$. Then, Line 14 initializes a CMM set R_1 as an empty set. Assume that vertex u of Q locates in the i^{th} row, $1 \le i \le |V_Q|$. Lines 16-17 enumerate all the possible mappings from vertices of B to u by assigning value 1 in different columns in the i^{th} row. Line 18 recursively calls Alg. 1 for the $(i+1)^{\text{th}}$ row's enumeration. If each row of C has been assigned with a value 1 (Line 10), Line 13 returns C as a CMM and then, Line 18 adds C into R_1. In particular, Line 11 checks in matrix C whether B's center w is mapped to any vertices of Q. If it is not, C is not a CMM of a candidate subgraph so that Line 12 returns an empty set. Finally, Line 20 returns R_1 as output.

EXAMPLE 4. *We illustrate Alg. 1 with the generation of the* CMM *C in Example 3. Lines 1-5 are initialization. For each query vertex u, Lines 6-9 obtain the vertex set $CV(u)$, i.e., $CV(u_1) = \{v_6\}$, $CV(u_2) = \{v_2, v_4\}$, $CV(u_3) = CV(u_4) = \{v_1, v_5, v_7\}$, and $CV(u_5) = \{v_3\}$. Lines 16-18 set $C(u_1, v_6) = 1$, $C(u_2, v_2) = 1$, $C(u_3, v_5) = 1$, $C(u_4, v_5) = 1$, and $C(u_5, v_3) = 1$ in turn to obtain C. Lines 10-13 return C as a* CMM *and Line 18 adds C into the set of all* CMMs.

Analysis. Alg. 1 is query-oblivious since its execution is only dependent of the vertex set V_Q but independent of the edge set E_Q. The detailed proof is presented in App. A.2 of [2]. For the time complexity, Lines 6-9 take $O(|V_Q| \cdot |V_B|)$ time. Lines 16-19 enumerate $O(\sum_{v \in V_Q} |CV(v)|^{|V_Q|})$ CMMs. The optimizations (Line 3) take negligible time compared to the whole enumeration process.

3.2 Query Verification

In this subsection, we present how to design a query-oblivious algorithm that verifies whether a CMM represents a valid match function under an *LGPQ* semantic. The main ideas are as follows.

Given a query Q with an *LGPQ* semantic $\mathcal{F}$, and a candidate subgraph G_c of graph G, the verification for matching V_Q to V_{G_c} under $\mathcal{F}$ is to detect no *matching violation*, *i.e.*, the unsatisfaction conditions w.r.t. $\mathcal{F}$'s definition. For example, for *hom*, a matching violation can be detected if there exists at least one edge e in Q that no edges in G_c can be matched to e (unsatisfaction on condition (2) of Def. 1). To detect the existence of such edges in Q on the Player side, we encode the existence of edges in M_Q as follows. We remark that this encoding is also applicable for *sub-iso* and *ssim* queries.

Encoding of M_Q (M_{Q_e}). $\forall\, i, j \in [1, |V_Q|]$,

$$M_{Q_e}(i,j) = \begin{cases} q, & \text{if } \overline{M_Q(i,j)} = 0; \text{ and} \\ 1, & \text{otherwise,} \end{cases}$$

where q is a large prime number and $\overline{M_Q(i,j)} = 1 - M_Q(i,j)$. Then, we present the query-oblivious verification algorithm for *hom*. (*sub-iso* can be supported with a minor modification [18].)

Algorithm 2: Query Verification Algorithm (*hom*)

Input : The encodings M_{Q_e} of query Q's adjacency matrix, the adjacency matrix M_G for graph G and a CMM C for matching V_Q to V_G

Output : An integer without factor q if C represents a valid match function under *hom* or a multiple of q, otherwise.

```
Procedure Verify(M_Qe, M_G, C):
1  r ← 1; //result initialization
2  M_p ← C · M_G · C^T; //M_p : G's adjacency matrix projected by C
3  foreach i ∈ [1, |V_Q|] do
4      foreach j ∈ [1, |V_Q|] do
5          if M_p(i, j) = 0 then
6              r ← r · M_Qe(i, j); //matching violation aggregation
7  return r;
```

Taking as inputs the encodings M_{Q_e} of query Q's adjacency matrix, the adjacency matrix M_G of graph G, and a CMM C for matching V_Q to V_G, Alg. 2 returns an integer without factor q if C represents a valid match function under *hom*. Otherwise, an integer with factor q is returned. In detail, Line 2 first computes the $|V_Q| \times |V_Q|$ adjacency matrix M_p of G that projects the vertices of G onto the vertices of Q according to C, where C^{T} denotes the transpose matrix of C. For each encoding $M_{Q_e}(i,j)$ (Lines 3-4), if $M_p(i,j) = 0$ (Line 5), it may lead to a matching violation on condition (2) of Def. 1 and hence Line 6 uses multiplication to aggregate $M_{Q_e}(i,j)$ into a result r. Line 7 returns r as output.

EXAMPLE 5. *Consider the query Q and graph G in Fig. 3 and the* CMM *C in Example 3. The encoding M_{Q_e} of M_Q is as follows: $M_{Q_e}(u_1) = (1,1,1,1,1)$, $M_{Q_e}(u_2) = M_{Q_e}(u_3) = (q,1,1,1,1)$, and $M_{Q_e}(u_4) = M_{Q_e}(u_5) = (1,q,1,1,1)$. In Alg. 2, Line 1 first set the value of r as 1. By using C and M_G, Line 2 computes the projected adjacency matrix M_p: $M_p(u_1) = (0,0,0,0,0)$, $M_p(u_2) = (1,0,0,0,0)$, $M_p(u_3) = M_p(u_4) = (1,1,0,0,0)$, and $M_p(u_5) = (0,1,0,0,0)$. For any i, j such that $M_p(i,j) = 0$ (i.e., $M_p(u_i, u_j) = 0$), Lines 3-6 aggregate $M_{Q_e}(i,j)$ into r by multiplication. Line 7 returns an r with value 1, which means that C represents a valid match function for Q under* hom. *Otherwise, a multiple of q is returned indicating that C does not represent a valid match function.*

Analysis. For any vertex u_i of the query Q and any vertex v_j of the graph G, we list all the possible cases of matching u_i to v_j. The correctness of Alg. 2 can be proved by summarizing its outputs of the matching cases that does not satisfy the requirements of the definitions of *LGPQ* semantics. Moreover, Alg. 2 is query-oblivious since its execution (Lines 2-5) depends on C and M_G, which are independent of the edge set E_Q. The detailed proofs are presented in App. A.2 of [2]. The encoding of M_Q can *be encrypted* by CGBE to preserve the query privacy while the query-obliviousness of Alg. 2 and the homomorphic computation supported by CGBE preserves the access pattern privacy. For the time complexity, assume both the addition and multiplication take $O(1)$ time. Then, the matrix multiplication in Line 2 takes $O(|V_G|^3)$ time and Lines 3-6 take $O(|V_Q|^2)$ time. In practice, $|V_G|$ equals the size of each candidate ball, which is limited by the diameter d_Q of the query.

Algorithm 3: Overall Algorithm of Prilo (*hom*)

Input : A query Q with V_Q, Σ_Q, L_Q, diameter d_Q and adjacency matrix $M^E_{Q_e}$ consisted of Q's encrypted encodings, and all balls of graph G
Output : The matching subgraphs of G for Q

On the Player **side:**
1 $R \leftarrow \emptyset$;
2 $l \leftarrow \arg\max_{l' \in \Sigma_Q} \{|\{v | v \in V_G \text{ and } L_G(v) = l'\}|\}$; //opt: choose label l
3 **foreach** $v_i \in \{v | v \in V_G \text{ and } L_G(v) = l\}$ **do** // ①: filter balls by l
4 $B_i \leftarrow G[v_i, d_Q]$, $r_i \leftarrow 0$; //①: filter balls by d_Q
5 $CS_i \leftarrow \text{CanEnum}(Q, v_i, B_i, 0, 0, \emptyset)$; //②: candidate enumeration
6 **foreach** $C \in CS_i$ **do**
7 $r_i \leftarrow \text{Verify}(M^E_{Q_e}, M_{B_i}, C) + r_i$; //③: query verification
8 $R \leftarrow R \cup \{r_i\}$;
9 send R to User;

On the User **side after** R **is received from** Players**:**
10 $R_H \leftarrow \emptyset$;
11 **foreach** $r_i \in R$ **do**
12 **if** the decrypted r_i does not have factor q **then** // ④: decrypt ciphertexts
13 retrieve the encrypted ball B_i from SP (Dealer); //⑤: retrieve ball
14 decrypt B_i's data by using the sk sent from DO; //⑥: decrypt ball
15 compute matching subgraphs B'_is of B_i for Q; //⑥: compute matches
16 $R_H \leftarrow R_H \cup \{B'_i\text{s}\}$;
17 **return** R_H;

3.3 Query Matching

In this subsection, we present the query matching step by the overall algorithm (Alg. 3) of the Prilo framework, as shown in Fig. 5.

• **On** Players**.** Taking a query with V_Q, Σ_Q, L_Q, diameter d_Q and the adjacency matrix $M^E_{Q_e}$ consisted of Q's encrypted encodings, and all balls of graph G as inputs, Alg. 3 outputs the matching subgraphs of G for Q. Recall that the candidate enumeration can choose arbitrarily a label l from Σ_Q and consider as candidate balls only those balls having centers of label l. Hence, as a simple optimization, Player ① first chooses a label l that maximizes the number of candidate balls in Line 2 after receiving the query Q from User. Then, Player ① filters balls of graph G by d_Q and l (Lines 3-4). For each candidate ball B, CMMs of all B's candidate subgraphs are ② enumerated in Line 5 (Sec 3.1) and ③ verified in Lines 6-7 (Sec. 3.2). Player sends to User the sets Rs of ciphertext results for all candidate balls of G in Line 9. We remark that the evaluations of balls are independent of each other and hence, can be readily parallelized.

• **On** User**.** The query matching step is as follows. User ④ decrypts the ciphertexts in the received ciphertext result set R (Lines 11-12). For each ciphertext r_i in R of ball B_i, if the decrypted r_i contains a factor q, B_i does not contain matching subgraphs for Q. Otherwise, User ⑤ retrieves the encrypted data of B_i from Dealer (Line 13) and decrypts B_i's data by using the secret key sk sent from DO (Line 14). Finally, User ⑥ computes the matching subgraphs of the retrieve balls for Q under the plaintext domain (Line 15) (*e.g.*, using any current state-of-the-art algorithms [27, 28, 40]) and outputs these subgraphs as query answers (Lines 16-17).

EXAMPLE 6. *The match function $\mathcal{H}$ in Example 3 is computed by Alg. 3 as follows. Line 2 chooses B as the label of l. Lines 3-8 evaluate those balls that i) have centers of label B, and ii) have diameters equal to $d_Q = 3$. Line 5 enumerates all the* CMMs *of ball $B = G[v_6, 3]$ by using Alg. 1. To compute r_i that indicates whether B contains valid match functions under* hom*, Lines 6-7 aggregate into r_i the outputs of Alg. 2 by addition for all the* CMMs *of B. In Example 5, Alg. 2's output for the* CMM *of $\mathcal{H}$ is* 1*. When taking as input the adjacency matrix $M^E_{Q_e}$ consisted of query Q's encrypted encodings but not the encodings M_{Q_e}, the output of $\mathcal{H}$ is r^n, where r (resp. n) denotes the random value of $M_{Q_e}(i, j)$ (resp. the number of multiplication) in Line 6 of Alg. 2. Therefore, there exists a decrypted r_i in Line 12 that does not have factor q, which encodes* 0 *(Sec. 3.2). On the* User *side, Line 13 retrieves the encrypted data of B, Line 14 decrypts the data, and Line 15 computes the matching subgraphs.*

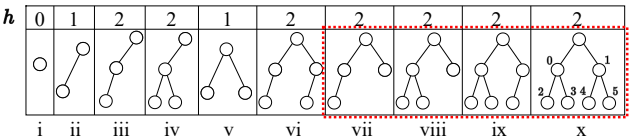

Figure 6: h-label binary trees ($h \leq 2$) (labels omitted)

Analysis. For the query matching step, although Dealer knows the specific balls retrieved by User (Line 13), Dealer cannot infer the edge information of the query from the encrypted ball data and hence, the query matching step is query-oblivious.

4 THE OPTIMIZED Prilo FRAMEWORK

To optimize Prilo, we propose an optimized framework called Prilo* that i) enables Players to detect as many as possible the *spurious* balls when preserving the privacy target and record them in the *pruning message*s (*PM*s) of balls (Secs. 4.1-4.2), and ii) enables User to *early* obtain the balls contain matching subgraphs by using these *PM*s (Sec. 4.3).

4.1 Bloom Filter of Trees in *TEE* (BF)

Different from existing works [18, 57] that compute the *PM*s by using simple graph topologies (*e.g.*, *neighbors* and *paths*), our first pruning technique, called BF, uses the *tree* topology. As reported in an analytical study of graph queries [8], for vertices of most queries, the average degree is smaller than 4 and the maximal degree is not larger than 5. Hence, we propose the *h-label binary trees* for detecting spurious balls.

DEFINITION 3. *(**h-label binary tree**) Given a height h, a graph G, and a vertex u of G, the* h-label binary tree $T_{u,h}$ *of G is a binary tree projected by the labels of nodes of an* undirected *binary subtree of G such that i) u is its root, ii) h is its height, and iii) For any two vertices v and v′ of this subtree, $v \neq v' \Rightarrow L_G(v) \neq L_G(v')$.*

We apply the undirected tree topology to detect more spurious balls since there may exist few directed trees in the queries having small sizes. Fig. 6 shows 10 possible topologies of h-label binary trees for $h \leq 2$ and we denote the h-label binary trees of such topologies by using a superscript i, $i \in \{\text{i}, ..., \text{x}\}$. For vertex u of the query in Fig. 3, Fig. 7 shows one $T^{\text{vii}}_{u,2}$ as an example. Then, we propose the following proposition for pruning.

PROPOSITION 3. *Consider a height h, a query Q, and a ball with the center w. If there exists at least one $T^i_{v,h}$, $i \in \{\text{i}, ..., \text{x}\}$ where v*

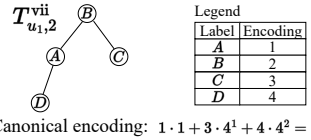

Figure 7: Example of 2-label binary tree of topology vii of Q in Fig. 3

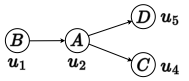

Figure 8: Example of h-twiglet of Q in Fig. 3 (where $h = 3$): $[B, A, [C, D]]$

Algorithm 4: Subtree Enumeration Algorithm

Input : The graph G and a vertex w of G
Output : The cases of enumerating subtrees of G for projecting $T^i_{w,2}$, $i \in \{\text{vii}, \ldots, \text{x}\}$

```
1  foreach neighbor u of w that L_G(u) ≠ L_G(w) do
2  |  start a BFS from u to obtain the set L(u);
3  foreach neighbor u of w that L_G(u) ≠ L_G(w) do // u: w's left child
4  |  foreach neighbor v of w that L_G(v) ≠ L_G(w) do // v: w's right child
5  |  |  CaseEnum(u, v, L);
   Procedure CaseEnum(u, v, L):
6  n_u ← |L(u) − {L_G(v)}|, n_v ← |L(v) − {L_G(u)}|;
7  if n_u = 1 then
8  |  TreeEnum(u, v, vii); //enumerate subtrees for T^vii_{w,2}
9  if n_u ≥ 2 then
10 |  foreach i ∈ {vii, viii} do
11 |  |  TreeEnum(u, v, i); //cases for T^vii_{w,2} and T^viii_{w,2}
12 |  if n_v = 1 then
13 |  |  TreeEnum(u, v, ix); //case for T^ix_{w,2}
14 |  if n_v ≥ 2 then
15 |  |  TreeEnum(u, v, x); //case for T^x_{w,2}
   Procedure TreeEnum(u, v, i):
16 enumerate subtrees of topology i by taking u as w's left child and v as w's right child ;
```

is a vertex of Q but there does not exist $T^i_{w,h}$ s.t. $T^i_{v,h}$ and $T^i_{w,h}$ are isomorphic, w cannot be matched to v under sub-iso, hom *and* ssim.

Prop. 3 can be established by a simple proof by contradiction of the definition of the *LGPQ* semantics. The detailed proof is presented in App. A.2 of [2]. Recall that B is spurious if B's center cannot be matched to any vertices of Q. Hence, for each vertex v of Q having the same label as B's center's label, we check Prop. 3. We consider B as spurious if $T^i_{v,h}$ *does* exist for all such vs and record the existence in a ciphertext c_{sgx} as one of the PM of B. In the following, we first present an algorithm to enumerate the 2-label binary trees and then present how BF securely computes the c_{sgx}.

4.1.1 Enumeration of 2-label binary trees. In Fig. 6, topologies i-ii and v (*resp.* vi) show labels of neighbors (*resp.* paths), whereas topology iv is a twiglet. For pruning purposes, we focus on four complex topologies (vii-x), shown within the red dotted rectangle. The enumeration algorithm is as follows.

Taking graph G and a vertex w of G as inputs, Alg. 4 enumerates the cases of all subtrees with root w and height 2 used to project $T^i_{w,2}$, $i \in \{\text{vii}, \ldots, \text{x}\}$. First, for each neighbor u of w, Lines 1-2 compute a label set $\mathcal{L}(u) = \{L_G(v) \mid v \in$ neighbors of u, $L_G(v) \neq L_G(u)$, $L_G(v) \neq L_G(w)\}$ for w's neighbors by using a *BFS*. Then, Lines 3-5 enumerate all subtrees with root w by taking all combinations of w's neighbors as w's two child nodes. In detail, for the left child u (*resp.* right child v) of w, Line 6 computes the number n_u (*resp.* n_v) of distinct labels of u's neighbors (*resp.* v's neighbors). As topologies vii-x shown in Fig. 6, if $n_u = 1$ (Line 7), only subtrees of topology vii can be enumerated (Line 8). Otherwise (Line 9), the subtrees of topologies vii-x are enumerated according to the value of n_v (Lines 10-15). Given w, u, v, and topology i, $i \in \{\text{vii}, \ldots, \text{x}\}$, Line 16 enumerates G's subtrees of topology i with height 2, which can be used to project $T^i_{w,2}$s.

EXAMPLE 7. *Take the graph G in Fig. 3 and G's vertex v_6 as inputs. The $T^{\text{vii}}_{v_6,2}$ in Fig. 7 can be enumerated by Alg. 4 as follows. First, for v_6's neighbors v_2, v_4 and v_5, Lines 1-2 compute $\mathcal{L}_Q(v_2) = \{C, D\}$, $\mathcal{L}_Q(v_4) = \{C\}$ and $\mathcal{L}_Q(v_5) = \{A\}$. By setting one neighbor (resp. another distinct neighbor) of v_6 as the left (resp. right) child u (resp. v) (Lines 3-4), Line 5 enumerates the $T_{v_6,2}$s. Given v_2 (resp. v_5) as u (resp. v), Line 8 enumerates the $T^{\text{vii}}_{v_6,2}$ shown in Fig. 7 since $n_{v_2} = 1$ and $n_{v_5} = 0$.*

Table 1: Numbers of 2-label binary trees for distinct topologies of ball B (d_{max}: the maximum degree of vertices of B)

Topology	No.s of 2-Label binary trees ($\kappa = \min\{|\Sigma_Q|, d_{max}\}$)
vii	$A^3_{\kappa-1}$
viii	$A^2_{\kappa-1} \cdot C^2_{\kappa-3}$
ix	$A^3_{\kappa-1} \cdot C^2_{\kappa-4}$
x	$C^2_{\kappa-1} \cdot C^2_{\kappa-3} \cdot C^2_{\kappa-5}$

Analysis. In Table 1, we present the maximum number of distinct 2-label binary trees of topologies vii-x in a ball, where C (*resp.* A) denotes the combination (*resp.* permutation) operator and d_{max} is the maximum degree of vertices of this ball. Regarding the time complexity of Alg. 4, Lines 1-2 take $O(V_G + E_G)$ time for *BFS*. Line 5 calls `CaseEnum` for $O({d_{max}}^2)$ times. In `CaseEnum`, Lines 7-15 call `TreeEnum` for $O(1)$ times. For `TreeEnum`, Line 16 takes at most $O({d_{max}}^4)$ time for enumerating subtrees of topology x with height 2. Therefore, Alg. 4's time complexity is $O\big(\max\{{d_{max}}^6, V_G + E_G\}\big)$.

4.1.2 Computation of c_{sgx}. To compute the c_{sgx} of a ball, we adopt the bloom filter to build a time- and space-efficient index used for securely checking the existence of query's 2-label binary trees by using the SGX. The 2-label binary trees are encoded as follows.

Canonical encoding of 2-label binary tree. Assume there is a *canonical encoding* of labels and 2-label binary trees such that *if* two trees are isomorphic, *then* their encodings are identical. Fig. 7 presents an example of converting one $T^{\text{vii}}_{u,2}$ into encoding. For the query Q in Fig. 3, where $|\Sigma_Q| = 4$, assume the encoding of labels A, B, C and D are 1, 2, 3 and 4, respectively. We propose further *each position in a topology has a unique index*, as shown in Fig. 6's topology x. From the label encoding and the index, we can compute that the canonical encoding[4] of the $T^{\text{vii}}_{u,2}$ in Fig. 7 is $1{\cdot}4^0 + 3{\cdot}4^1 + 4{\cdot}4^2 = 77$. Given a graph G, we can enumerate subtrees of topologies vii-x of G with height 2 by Alg. 4, and hence compute the encodings of their projected 2-label binary trees.

Query-oblivious computation. BF computes c_{sgx} as follows.

- **On** User**.** Given a query Q, User computes η encodings of distinct $T^i_{u,2}$s, $i \in \{\text{vii}, \ldots, \text{x}\}$ for each vertex u of Q, where η is a parameter used to i) ensure the query-oblivious checking, and ii) tune the false positive rates of bloom filters. If there are fewer than η encodings for u, User takes 0s as the rest encodings. If there are more than η encodings, User uses η encodings only, which may allow some false positives, so that some spurious balls cannot be detected. Such false positives do not affect the correctness of the pruning. Then, User encrypts these encodings (*e.g.*, by using *AES*) and sends them into SGXs' enclaves on Players by establishing secure channels.
- **On** Player **outside the enclave.** Given a ball B with the center w, Player i) computes the encodings of $T^i_{w,2}$, $i \in \{\text{vii}, \ldots, \text{x}\}$, ii) constructs a bloom filter for B by using these encodings with an encoding 0, and iii) transmits the bloom filter into the enclave.
- **On** Player **inside the enclave.** Inside the enclave, Q's encodings are decrypted when received. After B's bloom filter has been transmitted into the enclave, for each vertex u of Q having the same label

[4] For any two label nodes of a h-label binary tree T that i) they share the same parent, and ii) the unlabeled subtrees of T starting from them are isomorphic, we always put the node with a larger label encoding on the left to ensure a unique encoding of T.

Table 2: The 3-twiglet table $\mathcal{T}(u_1)$ of vertex u_1 of the query in Fig. 3, where $\Sigma = \{A, B, C, D\}$ and $L(u_1) = B$

3-twiglet ts in $\mathcal{T}(u_1)$	ciphertext c_ts	plaintext	meaning
$[B, A, C]$	$g^x rq$	0	exists
$[B, A, D]$	$g^x rq$	0	exists
$[B, A, [C, D]]$	$g^x rq$	0	exists
$[B, C, A]$	$g^x r$	1	not exists
$B, C, D]$	$g^x r$	1	not exists
$[B, C, [A, D]]$	$g^x r$	1	not exists
$[B, D, A]$	$g^x r$	1	not exists
$[B, D, C]$	$g^x r$	1	not exists
$[B, D, [A, C]]$	$g^x r$	1	not exists

as that of w, BF uses B's bloom filter to test whether u's η encodings exist in B. The tested results can be aggregated (*e.g.*, by addition) into an integer. The aggregated integer is encrypted as the c_{sgx} of B.

Analysis. The privacy analysis of BF is presented in Sec. 5. Regarding the bloom filter, the number of hash functions that minimizes its false positive rate (denoted by p) is $m/n \cdot \ln 2$, where m and n are the numbers of vector's bits and trees, respectively. Since the data transmission into SGX is known to be time-consuming, we focus on choosing the optimal value of parameter m. By some simple arithmetics on the number of trees listed in Table 1, we have the following equation,

$$m = -\frac{n \ln p}{(\ln 2)^2} < -4 \cdot \frac{\kappa^6}{2^3} \cdot \frac{\ln p}{(\ln 2)^2} < \frac{|V_Q|^6 \cdot \ln p}{-2 \cdot (\ln 2)^2} \quad (1)$$

With Eqa. 1, we can tune p to balance the data transmission cost and the pruning power of BF.

4.2 Query-Oblivious Twiglet Pruning

Without using the *TEE*, previous works check under the ciphertext domain the existence of simple topologies, *e.g.*, neighbors [17] and paths [57] of the query. If such topologies exist in the query but do not exist in a ball, this ball is considered as a spurious ball (Sec. 3.1). In this subsection, we propose using *twiglet*s to compute a ciphertext c_{phe} as another one of the *PM* of a ball.

First, we define *h-twiglet* as follows. Given a graph G, the *h-twiglet* of G is a topology consisted of labels of h+1 vertices of G, denoted by $\big[L_G(v_1), ..., L_G(v_{h-1}), [L_G(v_h), L_G(v_{h+1})]\big]$, $v_i \in V_G$, which satisfies the following: i) $(v_i, v_{i+1}) \in E_G$ or $(v_{i+1}, v_i) \in E_G$, $1 \le i \le h-2$, ii) $(v_{h-1}, v_h) \in E_G$ and $(v_{h-1}, v_{h+1}) \in E_G$, and iii) $\forall i, j \in [1, h+1]$, $i \ne j \Rightarrow L_G(v_i) \ne L_G(v_j)$. We denote such a topology as a h-twiglet t starting from v_1. Fig. 8 shows an example of 3-twiglet $\big[A, B, [C, D]\big]$ starting from u_1. Then, we have the following proposition.

PROPOSITION 4. *Consider a query Q and a ball B with the center w. For any vertex u of Q that having the same label as w's label, if there exists one h-twiglet in Q starting from u but there does not exist such h-twiglet in B starting from w, w cannot be matched to u under* hom*,* sub-iso*, and* ssim *semantics.*

Prop. 4 can be proved by contradiction of the definition of the *LGPQ* semantics. The detailed proof is presented in App. A.2 of [2]. For each vertex u of Q having the same label as the ball center w's label, we check the matching from w to u by using Prop. 4. If w cannot be matched to any vertices of Q, this ball is spurious. We illustrate the query-oblivious step for computing the c_{phe} by the twiglet pruning algorithm (Alg. 5).

- **On** User**.** Given a length h, for each vertex u of Q, User enumerates all the possible h-twiglets starting from u consisted of $|\Sigma_Q|$ labels and record them in a h-twiglet table of u. Take $h = 3$ and

Algorithm 5: Twiglet Pruning Algorithm `TwigletPrune`

Input : The length h, the encrypted h-twiglet table $\mathcal{T}$, and a ball B with the center w
Output : The ciphertext c_{phe} of B

```
1  Procedure TwigletPrune(T, M_B):
2  r ← 0;
3  start a DFS from w to find all h-twiglets in B and record them in a set R;
4  foreach u in Q that L_Q(u) = L_B(w) do
5      r' ← 1;
6      foreach h-twiglet t in T(u) do
7          if t ∈ R then
8              r' ← r' · c_1;                    // aggregate ciphertext of 1
9          else
10             r' ← r' · c_t;   // if violation, u has t but w doesn't
11     r ← r + r';
12 return r;
```

vertex u_1 in Fig. 8 as an example. Table 2 is a 3-twiglet table $\mathcal{T}(u_1)$ of u_1 where the first column of $\mathcal{T}(u_1)$ records *all* possible 3-twiglets starting from u_1. If a h-twiglet t in $\mathcal{T}(u)$ exists in Q, t is encoded and encrypted with 0 and $g^x rq$, respectively, where g, r and q are the generator of cyclic group, a random value and the predefined prime used in CGBE, respectively. The absence of t in Q is encoded and encrypted in $\mathcal{T}(u)$ as 1 and $g^x r$, respectively. User sends to Players the first two columns of all Q's vertices' 3-twiglet tables together with $Enc(Q)$ in ② of Fig. 4.

- **On** Players**.** After receiving the h-twiglet tables $\mathcal{T}$s, Player runs `TwigletPrune` (Alg. 5) to compute the c_{phe} for each ball. Taking h, $\mathcal{T}$s, and a ball B with center w as inputs, Alg. 5 outputs a ciphertext r as the c_{phe} of B. Line 3 first starts a *DFS* from w to find all the h-twiglets starting from w and record them in a set R. For each vertex u of Q having the same label as w's label (Line 4), Lines 5-11 aggregate into r the ciphertext r' for matching u to w. In detail, for each h-twiglet t in $\mathcal{T}(u)$ (Line 6), if there also exists t starting from center w in B (Line 7), Line 8 multiplies r' with a chosen ciphertext of 1 (denoted as c_1), which ensures the consistency of the power of the private key of CGBE for each r' in Line 11. This is to ensure the correctness of CGBE's decryption on User. If t does not exist in B (Line 9), whether w can be matched to u depends on the existence of t in Q, and hence, r' is multiplied by the ciphertext c_t of t in $\mathcal{T}(u)$ (Line 10). Line 11 aggregates all the r's into a ciphertext r, which indicates the existence of vertices of Q that may match w. If r is a multiple of q after decryption, w cannot be matched to any vertices of Q so that B is spurious. Line 12 returns r as the c_{phe} of B.

EXAMPLE 8. *Consider the query Q and graph G in Fig. 3. Taking length 3, the encrypted 3-twiglet table $\mathcal{T}$s of Q and the ball $B' = G[v_6, 3]$ of G as inputs, Alg. 5 computes c_{phe} of B' as follows. Since $L_Q(u_1) = L_G(v_6) = B$ (Line 4), Lines 5-11 check whether v_6 can be matched to u_1. Specifically, consider the first twiglet $[B, A, C]$ in $\mathcal{T}(u_1)$ as shown in Table 2. Since $[B, A, C]$ exists in B', Line 8 aggregates c_1 into r'. For the last twiglet $\big[B, D, [A, C]\big]$ in $\mathcal{T}(u_1)$, $\big[B, D, [A, C]\big]$ does not exist in $G[v_6, 3]$ and hence Line 10 aggregates $g^x r$ in r'. Finally, a ciphertext r', whose decrypted value has no factor q, is aggregated into r by addition. Since the decrypted c_{phe} of B' (i.e., the decrypted r) has no factor q, B' is not spurious.*

Analysis. In Sec. 5, we present Alg. 5 meets the privacy targets. Regarding the value of h, h=3 is used to covered label information of paths contained by topologies i-vi in Fig. 6. We assume $3 \le h \le 5$ for efficiency. For the complexity, Line 3 takes $O\big(|V_B| + |E_B|\big)$ time for *DFS* on ball B and hence, $O\big((|V_B| + |E_B|) \cdot {d_B}^2\big)$ time to enumerate all h-twiglets, where d_B is the maximum vertex degree of

B. The ciphertext aggregation (Lines 4-11) takes $O(|V_Q| \cdot A_{h-2}^{|\Sigma_Q|-1} \cdot C_2^{|\Sigma_Q|-h+1})$ time in the worst case, where C (*resp.* A) denotes the combination (*resp.* permutation) operator.

4.3 Secure Retrieval of Balls

Prilo* introduces a secure retrieval scheme into Prilo. The major steps of the scheme can be summarized as follows: 1) Players first compute the *PM*s of balls by using the pruning techniques in Secs. 4.1-4.2; 2) Dealer then generates sequences for Players to evaluate balls in their sequences, using techniques in Secs. 3.1-3.2, to obtain ciphertext results; and 3) From Dealer, User receives ciphertext results and retrieve the encrypted data of balls that contain matching subgraphs. We elaborate on the scheme in relation to ③-⑨ of Fig. 4 below.

On User**.** After ③ receiving the encrypted *PM*s (Secs. 4.1-4.2) from Players, User decrypts them. Given a $PM = (c_{sgx}, c_{phe})$ of a ball B, if the plaintext of either c_{sgx} or c_{phe} indicates that B is spurious, B is denoted as *negative*. Otherwise, B is denoted as *positive*. The information of whether B is negative ④ is sent from User to Dealer as B's decrypted *PM*. User waits for Dealer to ⑧ send the ciphertext results, and then decrypts them for ⑨ retrieving the encrypted data of balls that contains matching subgraphs.

On Dealer**.** After ④ receiving the set S of the ball identifiers (BIds) with their decrypted *PM*s, Dealer ⑤ generates for Player_i ($1 \le i \le k$, where k is the number of Players) a BId sequence $\mathcal{S}_i$ by using the *PM*s. $\mathcal{S}_i$ consisted of *a part of* BIds in S. The BIds of positives are *put in the front part of* $\mathcal{S}_i$ *in a query-oblivious manner*. After $\mathcal{S}_i$ ⑥ is sent to Player_i, Player_i conducts candidate enumeration and query verification (Secs. 3.1-3.2) for balls in $\mathcal{S}_i$. For each ball B evaluated on Player_i, Player_i ⑦ sends B's ciphertext result (r_i in Line 7 of Alg. 3) to Dealer *as soon as the evaluation on B finishes*. Dealer ⑧ sends the ciphertext results to User for decryption.

The scheme above enables User to i) find the balls containing matching subgraphs among positives early, ii) ⑨ retrieve the encrypted data of such balls from Dealer early, and iii) start computing the matching subgraphs early, while each Player_i may still be evaluating the rest of the balls in $\mathcal{S}_i$.

To ensure the privacy preservation of the retrieval scheme, *the key is to generate secure sequences of* BIds, so that each Player is *unaware* of the time when *all* its positives have been evaluated.

Secure sequence generation (SSG)**.** SSG has the set generation step and the ordering step, as illustrated with Fig. 9.

1) Set generation step. Given a BId set S and k Players, SSG i) generates a BId set S_i for Player_i ($1 \le i \le k$) that consists of two subsets, namely *early set* E_i and *dummy set* D_i, and then ii) orders the BIds in E_i and D_i to obtain sequences $\mathcal{E}_i$ and $\mathcal{D}_i$, and hence the BId sequence $\mathcal{S}_i = \mathcal{E}_i || \mathcal{D}_i$, where || is concatenation. The detailed generation of these two subsets can be described as follows.

- **Early set** (E)**.** Assume there are $|S| \cdot \theta$ ($0 \le \theta \le 1$) BIds of positives in S. Note that θ can be derived by the decrypted *PM*s and is *unknown* to Players. SSG partitions S into k early sets (E_i, $1 \le i \le k$) of the same size by assigning random $|S| \cdot \theta / k$ BIds of positives to E_i.
- **Dummy set** (D)**.** Given the early set E_i ($1 \le i \le k$), for each Player_i, SSG generates the dummy set D_i by assigning random $|S|/k$ BIds in $S - E_i$ to D_i, s.t. i) $\forall i \in [1,k]$, $E_i \cap D_i = \emptyset$, ii) $\forall i, j \in [1,k]$ ($i \ne j$), $D_i \cap D_j = \emptyset$, and iii) $D_1 \cup ... \cup D_k = S$. Note that SSG can simply generate $D_i = E_{(i+1) \bmod k}$, $1 \le i \le k$ when $k \ge 2$.

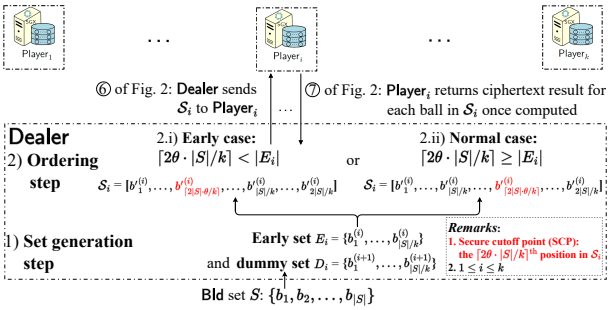

Figure 9: Steps of SSG: 1) The set generation step (bottom) uses the BId set S to generate S_i ($1 \le i \le k$), which consists of the early set E_i and dummy set D_i. 2) The ordering step generates a sequence $\mathcal{S}_i$ for Player_i by using E_i and D_i, and orders the BIds in $\mathcal{S}_i$. Depending on the ratio θ of positives to all balls in S, there are two ordering cases: i) early case ($\theta < 1/2$), and ii) normal case ($\theta \ge 1/2$).

2) Ordering step. The length of sequence $\mathcal{S}_i$ ($1 \le i \le k$) to be generated by SSG for Player_i is $|\mathcal{S}_i| = |E_i| + |D_i| = 2 \cdot |S|/k$. We denote the $\lceil 2\theta \cdot |S|/k \rceil^{\text{th}}$ position in $\mathcal{S}_i$ as the *secure cutoff point* (SCP) and use SCP to help ordering BIds, such that all positives of S_i would have been evaluated by Player_i when Player_i finishes the evaluation of the ball located on SCP. The ordering has two cases.

- **i) Early case** ($\theta < 1/2$)**.** As Fig. 9 shows, SCP resides in the front half part of $\mathcal{S}_i$ since $\lceil 2\theta \cdot |S|/k \rceil < |S|/k \rceil = |E_i|$. W.l.o.g, assume that $y = \lceil 2\theta \cdot |S|/k \rceil$ and y is even. For Player_i ($1 \le i \le k$), SSG i) randomly chooses $y/2$ BIds of negatives in E_i, ii) inserts into a set E_i' the chosen $y/2$ BIds together with the BIds of all the $y/2$ positives in E_i, and iii) orders the BIds in E_i' (*resp.* $(E_i - E_i') \cup D_i$) with a random sequence to obtain the sequence $\mathcal{E}_i$ (*resp.* $\mathcal{D}_i$). Then, $\mathcal{S}_i = \mathcal{E}_i || \mathcal{D}_i$.
- **ii) Normal case** ($\theta \ge 1/2$)**.** SCP resides in the rear half part of $\mathcal{S}_i$ since $\lceil 2\theta \cdot |S|/k \rceil \ge |S|/k \rceil = |E_i|$. In this case, SCP cannot lead to an early return of positives' ciphertext results to User. Hence, SSG simply applies a random sequence generation (denoted by RSG), which i) randomly partitions S into k subsets of the same size (for simplicity, assume $|S|$ is divisible by k), and ii) randomly orders the BIds in the subsets to obtain sequences for Players. Note that the value of θ depends on the pruning power of our proposed pruning techniques in Secs. 4.1-4.2.

EXAMPLE 9. *We illustrate* SSG *by an example. Consider* $k = 3$ Players *and a* BId *set* $S = \{b_1, b_2, b_3, b_4, b_5, b_6, b_7, b_8, b_9\}$. *Assume* b_5, b_6 *and* b_7 *are* BIds *of positives. Hence,* $\theta = 3/9$ *and* SCP *is the* 2^{nd} *position. Then,* SSG *generates subsets* $E_1 = \{b_8, b_2, b_5\} = D_2$, $E_2 = \{b_6, b_1, b_9\} = D_3$ *and* $E_3 = \{b_7, b_3, b_4\} = D_1$. *With these subsets,* SSG *generates* BId *sequences* $\mathcal{S}_1 = [b_5, b_8] \,||\, [b_9, b_2, b_1, b_6]$, $\mathcal{S}_2 = [b_6, b_1] \,||\, [b_4, b_7, b_9, b_3]$ *and* $\mathcal{S}_3 = [b_3, b_7] \,||\, [b_2, b_5, b_8, b_4]$. *Dealer can receive the ciphertext results of all positives when* b_8 *in* $\mathcal{S}_1$, b_1 *in* $\mathcal{S}_2$, *and* b_7 *in* $\mathcal{S}_3$ *have been evaluated by* Player_1, Player_2, *and* Player_3, *respectively.*

We remark that θ and SCP are not known to Players and Players have no way to identify the case and therefore the positives. The privacy analysis of SSG is presented in Sec. 5. With the sequences

generated by SSG, User can receive the ciphertext results of all positives before the end of the whole query processing of Prilo on Players. After decrypting the ciphertexts, User identifies the balls containing matching subgraphs and sends to Dealer the BIds of these balls for retrieving their encrypted ball data to decrypt and to compute the matching subgraphs.

5 PRIVACY ANALYSIS

Due to space restrictions, we present the main ideas of the privacy analysis in this section, and provide the detailed proofs in App. B [2]. We recall that the privacy target (Sec. 2.3) consists of i) the query privacy, and ii) the access pattern privacy. We start with Prop. 5.

PROPOSITION 5. *Given a query Q, i) the encrypted encodings $M^E_{Q_e}$ of Q's adjacency matrix, ii) the twiglet tables $\mathcal{T}$s, and iii) the encrypted encodings of 2-label binary trees of Q's vertices are preserved from* SP *against the attack model.*

Since $M^E_{Q_e}$ and $\mathcal{T}$ (*resp.* the encrypted encodings of Q's 2-label binary trees) are encrypted by CGBE (*resp. AES*), they are protected from Players. These encrypted messages are protected from Dealer since Dealer i) does not have the private key of CGBE and *AES*, and ii) cannot obtain these encrypted messages due to the assumption that Dealer and Players do not collude (Sec. 2.3). Prop. 5 holds.

For the Prilo framework, we have i) Algs. 1-3 are *query-oblivious* (as shown in the analyses in Sec. 3) that preserves the access pattern privacy, and ii) the encryption used in Algs. 1-3 preserves the query privacy [17]. Hence, we can derive Prop. 6 as follows.

PROPOSITION 6. *The privacy target is preserved by the* Prilo *framework from* SP *against the attack model.*

Regarding the BF pruning, the bloom filter always tests $O(\eta)$ encodings (η is a parameter set by User) inside SGX's enclave (Sec. 4.1.2). BF is query-oblivious since η is independent of the edge set of the query. The enclave preserves the privacy of the plaintexts of these encodings. The size of each bloom filter is smaller than $4KB$ under our experimental settings (Sec. 6.1). Hence, the granularity of the memory access pattern attacks on the enclave becomes finer that "*the attackers become harder to get valid information*" [26]. Putting these ideas together, we have Prop. 7.

PROPOSITION 7. *The privacy target is preserved by the* BF *pruning from* SP *against the attack model.*

Regarding the twiglet pruning (in Sec. 4.2), let $\mathcal{G}(\mathcal{T}, i)$ (*resp.* $\mathcal{G}(r)$) be a function that returns 1 if SP can compute the corresponding plaintext of ciphertext c_{t_i} of h-twiglet t_i in $\mathcal{T}$ (*resp.* the output ciphertext r of Alg. 5) and returns 0, otherwise. Then, we quantify the probability that SP can attack r (*i.e.*, $\mathcal{G}(r) = 1$) after applying twiglet pruning, as presented in Prop. 8.

PROPOSITION 8. *After running* `TwigletPrune`, $Pr[\mathcal{G}(r) = 1] \leq 1/2^n + \epsilon$, *where n is the number of ciphertexts c_ts aggregated into r in Line 10 of Alg. 5 and ϵ is a negligible value.*

$Pr[\mathcal{G}(r) = 1]$ equals the product of $Pr[\mathcal{G}(\mathcal{T}, i) = 1]$ for the n t_is used in `TwigletPrune`. As t_is are encrypted by CGBE (secure against *CPA* [17]), we have $Pr[\mathcal{G}(\mathcal{T}, i) = 1] \leq 1/2 + \epsilon'$ (ϵ' is a negligible value) which has a negligible difference from random guessing. Prop. 8 holds. Moreover, Lines 6-11 of Alg. 5 are independent of the edge set of the query that `TwigletPrune` is query-oblivious, we have established Prop. 9.

PROPOSITION 9. *The privacy target is preserved by the twiglet pruning from* SP *against the attack model.*

Regarding SSG (Sec. 4.3), Dealer knows i) the decrypted pruning messages (*PM*s) and ball identifiers (BIds) of the balls sent from User, and ii) the ciphertext results sent from Players. However, Dealer has only the encrypted ball data without i) the secret key for ball data's decryption, and ii) the private key of CGBE for decrypting ciphertext results. Dealer cannot infer the query structure by using such information. For Players, each Player_i knows only the BId sequence $\mathcal{S}_i$ without the plaintexts of the *PM*s. The probability that a Player can determine whether a ball in $\mathcal{S}_i$ is spurious is smaller than $1/2 + \epsilon$, where ϵ is a negligible value (see App. B.4 of [2] for details). Hence, the access pattern privacy is preserved by SSG from Players. The query privacy is also preserved by SSG from Players since each Player_i knows only the ball data and sequence $\mathcal{S}_i$ without the plaintexts of the *PM*s when evaluating the balls in $\mathcal{S}_i$. With the assumption that Dealer and Player do not collude, we have Prop. 10.

PROPOSITION 10. *The privacy target is preserved by* SSG *from* SP *against the attack model.*

By putting Props. 5, 6, 7, 9 and 10 together, we have Theorem. 1.

THEOREM 1. Prilo* *preserves the privacy target from* SP *against the attack model.*

6 EXPERIMENTAL EVALUATION

In this section, we evaluate the efficiency of Prilo* and the effectiveness of the proposed pruning techniques.

6.1 Experimental Settings

Platform. We implemented the prototype of Prilo* in C++ using a machine with an Intel Core i7-7567U 3.5GHz CPU and 32GB RAM running Ubuntu 20.04.4 LTS with Intel(R) SGX SDK[5] to test the performance for both User and SP (including multiple Players and a Dealer). CGBE was implemented by using the *GMP* libraries.

Datasets and query sets. We used three real-world datasets, namely *Slashdot*, *DBLP*, and *Twitter* [34], which are also used in [18, 53, 57, 61]. The vertices of these datasets do not have labels. Similar to existing works [18, 40, 57], we generated a random label for each vertex to evaluate Prilo*'s performance. We focused on *hom* and *ssim* queries, but omitted *sub-iso* queries, as the performance is similar to that of *hom* queries. Table 3 shows the statistics of these datasets, where $|\Sigma^H_G|$ (*resp.* $|\Sigma^S_G|$) is the size of label set for *hom* (*resp. ssim*) queries, whose value was set according to [18, 57]. Regarding the query sets, we used the same query generator *QGen* [57]. We generated 10 random queries for each experiment. Taking a query size $|V_Q|$, a diameter d_Q and a graph G as inputs, *QGen* returned random subgraphs of G as output queries. The default values of $|V_Q|$ and d_Q were 8 and 3, respectively. Table 4 shows the statistics of balls evaluated on Players under the default setting. For each ball B, we used the size of B's vertex set, $|V_B|$, as the *ball size* of B.

Default parameters. These parameters are described as follows:

[5] https://github.com/intel/linux-sgx#license

Table 3: Statistics of three real-world datasets

Graph G	$\|V_G\|$	$\|E_G\|$	$\|\Sigma_G^H\|$	$\|\Sigma_G^S\|$
Slashdot	82,168	948,464	100	64
DBLP	317,080	1,049,866	150	64
Twitter	81,306	1,768,149	100	64

Table 4: Statistics of candidate balls Bs for 10 random queries under the default setting

Graph	Avg. no. of balls per query	avg. $\|V_B\|$	stddev. of $\|V_B\|$	avg. $\|E_B\|$	stddev. of $\|E_B\|$	Max. degree
$Slashdot_{100}$	204	243	218	1085	1062	333
$Slashdot_{64}$	3383	580	538	3324	3325	689
$DBLP_{150}$	18	25	11	34	25	20
$DBLP_{64}$	3001	45	38	66	64	38
$Twitter_{100}$	378	245	245	822	854	214
$Twitter_{64}$	5734	467	495	2113	2344	398

• CGBE. The encoding q and random number r for CGBE were both of 32 bits and the public value was of 4096 bits [57].
• *Query*. The default values of $|V_Q|$ and query diameter d_Q were 8 and 3, respectively. We set $d_Q = 4$ to investigate the pruning power of h-twiglet by varying h from 3 to 5.
• BF *pruning* (BF). For the parameter η used to ensure BF's obliviousness, we set $\eta = 256$. In practice, the number n of distinct 2-label binary trees starting from a ball's center is much smaller than $|V_Q|^6/2$, in particular, $n \leq 10K$ for almost all our experiments. Hence, we set $n = 10K$ and the desired false positive rate $p = 0.3$, and $m = 25K$ bits are required for the bloom filter by Eqa. 1. Compared with passing $25K$ bits of data between the enclave and the application of SGX, BF's online construction of bloom filters for ball centers may take more time, especially for the enumeration of subtrees of topology x (Lines 14-15 of Alg. 4). Hence, we used a threshold t for BF to balance the efficiency and pruning performance. Specifically, for the ball center, if there exist more than t neighbors whose $\mathcal{L}$ (Line 2 of Alg. 4) has size larger than 3, BF simply marked the ball as positive. We varied t = 5, 15, or 25 for BF and denoted the corresponding algorithm as $\mathtt{BF}_t$. The default value of t was 15.
• *Twiglet pruning* (Twiglet). We pruned balls using i-twiglets, $3 \leq i \leq h$, where the hop length h ranged from 3 to 5. We use a h value to denote Twiglet as $\mathtt{Twiglet}_h$. The default value of h was 3.
• *Path-based pruning* (Path) [57]. We used the existing path-based pruning technique as the baseline for comparison. We denote Path using a h value as $\mathtt{Path}_h$.
• *Number of* Players. The number of Player servers is denoted by k, where k = 4, 8, or 16. The default value of k was 4.

6.2 Overall Performance

We first investigate the overall performance of some computations on the User side, BF & Twiglet, and Prilo*.

EXP-1. Performance on the User **side**. User i) generates the encrypted messages for queries, ii) decrypts the pruning messages, and iii) decrypts the ciphertext results sent from Dealer.
• *Preprocessing*. Given a query Q, User generated the encrypted encoding $M_{Q_e}^E$ of Q's adjacency matrix, a twiglet table $\mathcal{T}$ and the encrypted encodings of 2-label binary trees for each vertex of Q. The total preprocessing time was always less than 0.25s, including *AES256*'s encryption for the encodings of 2-label binary trees to be sent to the enclave and CGBE's encryption for i) the encoding M_{Q_e}, ii) the $\mathcal{T}$s, and iii) the value 1 to obtain a chosen ciphertext c_1 used for Twiglet (Line 8 of Alg. 5).
• *Decryption*. User decrypted the ciphertexts returned by BF (Sec. 4.1.2), Twiglet (Alg. 5) and Prilo (Alg. 3). The total decryption time under our experiments was always less than 0.5s only.
• *Message sizes*. Given query Q and h used for Twiglet, User sent to Players i) $\eta \cdot |V_Q|$ encodings of 2-label binary trees encrypted by *AES256*, and ii) the $M_{Q_e}^E$ and encrypted $\mathcal{T}$s which contained $|V_Q|^2$ and $|V_Q| \cdot P_{h-1}^{|\Sigma_Q|-1} \cdot C_2^{|\Sigma_Q|-h}$ ciphertexts encrypted by CGBE, respectively. For Player_i, where $1 \leq i \leq k$ on the SP side, Algs. 4 and 5 returned $O(\mathcal{N}_i)$ ciphertexts to be sent to User, where $\mathcal{N}_i$ is the number of balls evaluated on Player_i. Take the queries used for *Twitter* in **EXP-2** as an example, the size of $M_{Q_e}^E$ and encrypted $\mathcal{T}$s under our experimental settings were at most $k \times 8MB$, where k is the number of Players. The size of encodings encrypted by *AES256* is smaller than 10MB. The total size of messages sent from Players to User was no larger than 20MB only.

EXP-2. Overall runtimes of $\mathtt{BF}_{15}$ and $\mathtt{Twiglet}_3$. We investigate the efficiency of BF and Twiglet under the default setting. Due to space restrictions, we report only the results when the figures and detailed analysis are presented in App. C of [2]. $\mathtt{BF}_{15}$ took hundreds of milliseconds for *hom* queries and few seconds for *ssim* queries, respectively. Not surprisingly, the runtimes of $\mathtt{BF}_{15}$ on all datasets increase as the ball sizes increase. The runtimes of $\mathtt{Twiglet}_3$ on *Slashdot* and *Twitter* increase slightly as the ball sizes increase when $\mathtt{Twiglet}_3$'s runtime on *DBLP* is not sensitive to the ball size.

EXP-3. Overall performance of Prilo*. The following average results were from 10 random queries under the default setting. In Fig. 10, *All* denotes the average number of candidate balls, which can be either positive or negative. Fig. 10 reports the average number of candidate balls after pruning negatives by each method. Although $\mathtt{BF}_{15}$ pruned fewer negatives than $\mathtt{Twiglet}_3$ or $\mathtt{Path}_3$, $\mathtt{BF}_{15}$ helped $\mathtt{Twiglet}_3$ to further prune negatives, especially for *ssim* queries.

In Fig. 11, we denote Steps ⑤-⑦ of Fig. 4 of Prilo* by using SSG (*resp.* a baseline that applies RSG for both cases of SSG) as SSG (*resp.* RSG), and denote the times for Dealer to obtain the ciphertext results of positives as their runtimes. Fig. 11 shows the average total runtimes of (i) $\mathtt{BF}_{15}$, $\mathtt{Twiglet}_3$, and $\mathtt{Path}_3$, and (ii) SSG and RSG for both the *hom* and *ssim* queries.[6] First, it can be observed that the runtimes of $\mathtt{BF}_{15}$, $\mathtt{Twiglet}_3$, and $\mathtt{Path}_3$ are very small. We can see that the runtimes of the pruning methods ($\mathtt{BF}_{15}$, $\mathtt{Twiglet}_3$, and $\mathtt{Path}_3$) for *hom* queries are much smaller than the ones for *ssim* queries due to fewer candidate balls. Next, by comparing the runtimes of SSG and RSG, we can better present the performance of the optimization in Sec. 4.3. The runtime of SSG is often one order of magnitude smaller than the runtime of RSG. Regarding the runtime for User to start receiving from Dealer the ciphertext results of non-spurious balls,[7] the runtime of Prilo* equals the sum of the runtimes of BF, Twiglet and SSG while the runtime of Prilo equals that of RSG. For example, the average runtimes of Prilo* and Prilo on *Twitter* are 6.8 + 2.4 + 7.5 = 16.7 and 63.8, respectively. The runtimes of Prilo* was either much smaller than or similar to that of Prilo, which verified the effectiveness of Prilo*.

[6] To save the runtime, the balls that obviously involve numerous candidate enumeration simply bypass the pruning.
[7] We omitted the evaluation on User to compute the detailed subgraphs by using the state-of-the-art *LGPQ* matching algorithms [27, 28, 40] under the plaintext domain.

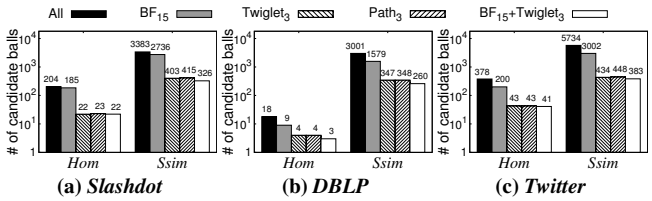

(a) *Slashdot* (b) *DBLP* (c) *Twitter*

Figure 10: Average number of candidate balls for algorithms

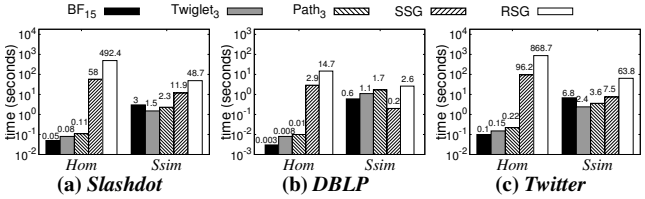

(a) *Slashdot* (b) *DBLP* (c) *Twitter*

Figure 11: Average total runtimes for algorithms

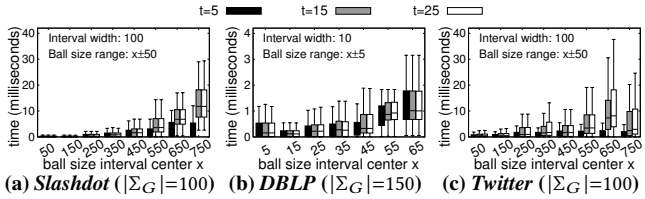

(a) *Slashdot* ($|\Sigma_G|$=100) (b) *DBLP* ($|\Sigma_G|$=150) (c) *Twitter* ($|\Sigma_G|$=100)

Figure 12: Per-ball runtimes by varying t for $\mathtt{BF}_t$

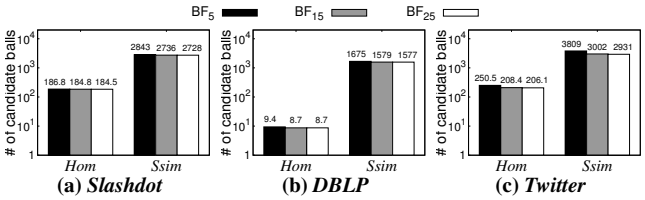

(a) *Slashdot* (b) *DBLP* (c) *Twitter*

Figure 13: Average number of candidate balls by varying t for $\mathtt{BF}_t$

6.3 Effects of Varying Settings

To investigate the performance of the algorithms, we ran them by varying one parameter at a time while keeping the other parameters to their default values. It is known that the numbers of balls to be evaluated vary with queries. Hence, for ease of presentation, we used boxplots to present the runtimes.[8] The following figures do not display the outliers (fewer than 1%).

EXP-1. Varying t for $\mathtt{BF}_t$. Fig. 12 shows that $\mathtt{BF}_t$'s runtimes increase as t increases until t's value reaches 15. The reason is that most ball centers of these datasets have fewer than 15 neighbors vs of the ball center that $|\mathcal{L}(v)| \geq 3$ and hence decreasing t's value can hardly reduce the runtime of $\mathtt{BF}_t$ when $t \geq 15$. From Fig. 13, we see that $\mathtt{BF}_t$ with a larger t prunes more negatives and $t = 15$ reaches a balance between the efficiency and pruning power of $\mathtt{BF}_t$.

EXP-2. Varying h for $\mathtt{Twiglet}_h$. As Fig. 14 shows, the runtimes of $\mathtt{Twiglet}_h$ increase as h increases since a larger h requires more time for *DFS* in $\mathtt{Twiglet}_h$ to obtain the i-twiglets, $3 \leq i \leq h$. In Fig. 14(b), $\mathtt{Twiglet}_h$'s runtimes on *DBLP* vary a lot for balls of small sizes. This is because the number of twiglets enumerated for small balls varies a lot.

[8] In x-axis, we grouped the balls according to their sizes. Only 1% of balls were beyond the x range. The box of each interval was drawn around the region between the first and third quartiles, and a horizontal line at the median value. The whiskers extended from the ends of the box to the most distant point with a runtime within 1.5 times the interquartile range. Points that lie outside the whiskers were outliers.

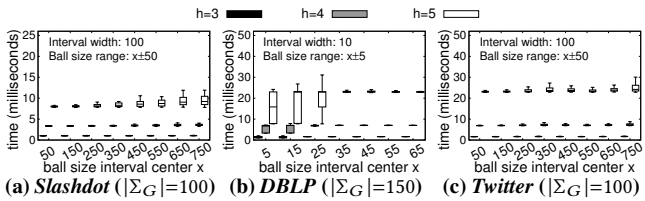

(a) *Slashdot* ($|\Sigma_G|$=100) (b) *DBLP* ($|\Sigma_G|$=150) (c) *Twitter* ($|\Sigma_G|$=100)

Figure 14: Per-ball runtimes by varying h for $\mathtt{Twiglet}_h$

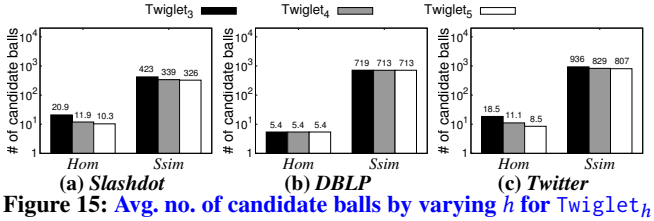

(a) *Slashdot* (b) *DBLP* (c) *Twitter*

Figure 15: Avg. no. of candidate balls by varying h for $\mathtt{Twiglet}_h$

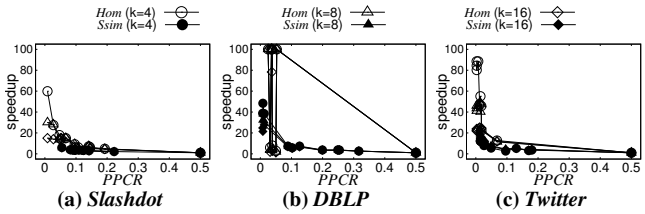

(a) *Slashdot* (b) *DBLP* (c) *Twitter*

Figure 16: Prilo*'s speedup by varying *PPCR*

Fig. 15 shows that $\mathtt{Twiglet}_h$ with a larger h can prune more negatives by using more twiglets. However, the improvement in pruning is not obvious since there are few i-twiglets where $i > 3$. In practice, the default value 3 for h demonstrates a good balance between the efficiency and the pruning power.

EXP-3. Varying k for Players. In Fig. 11, we use the runtimes of SSG and RSG to present the efficiency of Prilo*. As shown in Sec. 4.3, the runtime of SSG is related to the value of θ, which depends on the pruning power of BF and Twiglet. Note that θ is also defined as the *predicted positive condition rate* (*PPCR*), *i.e.*, $(TP + FP) / (TP + TN + FP + FN)$, where TP (*resp.* TN) denotes *true positive* (*resp. true negative*), and FP (*resp.* FN) denotes *false positive* (*resp. false negative*), respectively. Thus, we use *PPCR* to present the pruning powers of our proposed methods.

In Fig. 16, we use the ratio of RSG's runtime to SSG's runtime (*i.e.*, Prilo*'s speedup) as the y-axis and *PPCR* as the x-axis to present Prilo*'s improvement in efficiency when varying the number k of Players. For presentation purpose, we cap the speedup at 100. Given large *PPCR*s, we can observe that the speedup is not sensitive to k. However, for small *PPCR*s, the speedup decreases when k increases. This is because the number of positives is relatively small that increasing the number of Players cannot return the positives' results to User earlier. In Fig. 16(b), the speedup varies a lot for *hom* queries on *DBLP* due to the variation in Prilo*'s runtime on few candidate balls, where there is only 1 positive for most queries.

Fig. 17 shows the runtimes of SSG for both *hom* and *ssim* queries when k varies. We can see that SSG's runtime decreases when k increases. When *PPCR* is small, more Players cannot decrease SSG's runtime as there are few positives. Similar to Fig. 16(b), in Fig. 17(b), SSG's runtimes for *hom* queries on *DBLP* vary a lot for small *PPCR*s.

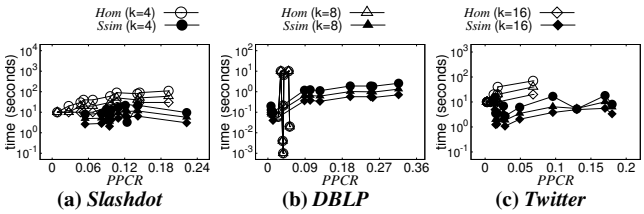

(a) *Slashdot* (b) *DBLP* (c) *Twitter*

Figure 17: Runtimes of SSG by varying *PPCR*

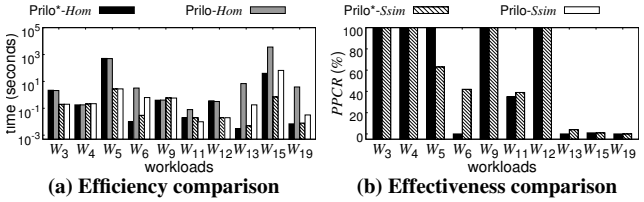

(a) Efficiency comparison (b) Effectiveness comparison

Figure 18: Performance of 10 workloads derived from *LDBC*

6.4 Experiments on *LDBC* Workloads

We investigated Prilo*'s performance on the *LDBC* workloads [1].

***LDBC* social network dataset.**[9] We used the value of *tag-class* as the label of each vertex. The transformed graph with scale factor 1 has 3,156,275 vertices, 10,375,137 edges and 213 labels.

Queries. To derive *LGPQ* queries from practical workloads, we made a few simplifications: We omitted the value predicates (*e.g.*, *date* and *name*) of vertex label, reachability queries, negations, trivial structures (*e.g.*, single edge), and well-known relationships (*e.g.*, between "*city*" and "*country*"). Then, we obtained the structures of 10 out of 20 business intelligence workloads. Some characteristics of the workloads are reported in App. C of [2]. For each workload pattern, we generated a query by randomly assigning a label to each query vertex by using the *tag-class* of *LDBC* [1].

For presentation clarity, we report the efficiency and effectiveness under *hom* and *ssim* semantics in Figs. 18(a) and 18(b). It can be observed from Fig. 18(a) that, for queries W_3, W_4, W_5, W_9 and W_{12}, the runtimes of Prilo* and Prilo are similar. This is because these queries have simple patterns (*e.g.*, 2-hop path) that few spurious balls can be detected by Prilo*. The *PPCR*s for these queries are larger than 0.5 as shown in Fig. 18(b) and hence, Prilo* applies RSG, as Prilo does. For W_6 under *ssim*, although the *PPCR* is slightly smaller than 0.5, Prilo*'s speedup is larger. This is because the sizes of the non-spurious balls are much smaller than the sizes of the spurious ones. For the rest queries, Prilo*'s speedup is obvious due to small *PPCR*s.

7 RELATED WORK

Privacy preserving queries. There have been works on privacy preserving query processing [5, 15, 33, 53, 55, 62] in recent years. For graph pattern queries, three kinds of privacy models are studied. The difference between these models resides in the privacy target about the following structure(s).

• *Both query and data graph*: Cao et al. [10] studied tree pattern queries on encrypted *XML* documents by predetermining the traversal order for each query. Cao et al. [11] proposed a *filtering and verification* method to solve the *sub-iso* query over encrypted graph-structured data in cloud computing. Fan et al. [17] also studied the *sub-iso* query semantic and proposed the *cyclic group based encryption scheme* (CGBE) to determine only the existence of matching subgraphs. They did not consider ball retrieval.

• *Data graph only*: By utilizing the *k-automorphic graph*, Chang et al. [12] and Huang et al. [25] studied the *sub-iso* query semantic, while Gao et al. [19] studied the *strong simulation* query [40]. In this model, users' queries are known by SP.

• *Query only*: By using CGBE, Fan et al. [18] only answered *Yes/No* to the existence of matching subgraphs for the *sub-iso* query, while Xu et al. [57] studied the problem of the *ssim* query and only sketched a trivial baseline for retrieving the matching subgraphs.

Cryptosystem. The asymmetric scalar-product-preserving encryption scheme (*ASPE*) [54] was used in [17] to compute the pruning messages securely. However, [60] has proved that *ASPE* is insecure under the known plaintext attack (*KPA*). Boneh-Goh-Nissim (*BGN*) [7] is a cryptosystem that supports somewhat homomorphic computation on ciphertexts. However, the performance of the SOTA *BGN* [23] is still impractical in our case. We proposed a twiglet pruning technique by applying *CGBE* [17] to aggregate the key ciphertexts since *CGBE* supports efficient homomorphic operations.

Secure query framework. Gentry et al. [20] described the first plausible construction for a fully homomorphic encryption (*FHE*) that supports both addition and multiplication on ciphertexts. Due to the known poor performance, *FHE* cannot be adopted. An oblivious *RAM* simulator (*ORAMs*), introduced by Goldreich et al. [21], is a compiler that transforms algorithms in a way that the resulting algorithms preserve the input-output behavior of the original algorithm but the distribution of memory access pattern of the transformed algorithm is independent of the memory access pattern of the original algorithm. However, *ORAMs* cannot be adopted since the query cannot be known to SP. *GraphSC* [42], *GraphSE*^{2} [31] and *PeGraph* [52] are frameworks for privacy preserving query on encrypted graph data, which also need the query structure for the matching process. The trusted execution environment (*TEE*) is a recent solution for databases [51, 56, 63]. The security is guaranteed by the hardware.

8 CONCLUSION

This paper proposes Prilo* for the problem of privacy preserving *localized graph pattern query* (*LGPQ*) processing in a cloud computing paradigm. Prilo* is a general framework that can handle *subgraph isomorphism*, *subgraph homomorphism*, and *strong simulation* semantics, where their query results are localized in subgraphs called balls. Moreover, Prilo* presents a BF pruning technique that exploits a *trusted execution environment* and a twiglet-based pruning technique under the ciphertext domain to securely compute the pruning messages of balls of the data graph. Based on these pruning messages, Prilo* proposes a ball retrieval scheme to enable User to privately retrieve from the service provider the balls that contain results early and hence, compute the query results early. Privacy analysis results and proof sketches are presented. The experimental results have shown the efficiency of Prilo*. As for future work, we plan to apply Prilo* to other *LGPQ*s, such as *p-homomorphism* query [47] and *conditional graph pattern* (*CGP*) query [16].

[9] https://ldbcouncil.org/benchmarks/snb/

REFERENCES

[1] Renzo Angles, János Benjamin Antal, Alex Averbuch, Altan Birler, Peter Boncz, Márton Búr, Orri Erling, Andrey Gubichev, Vlad Haprian, Moritz Kaufmann, et al. 2020. The LDBC social network benchmark. *arXiv* (2020).

[2] Anonymity. 2022. https://anonymous.4open.science/r/LGPQ-0129.

[3] Sergei Arnautov, Bohdan Trach, Franz Gregor, Thomas Knauth, Andre Martin, Christian Priebe, Joshua Lind, Divya Muthukumaran, Dan O'keeffe, Mark L Stillwell, et al. 2016. {SCONE}: Secure linux containers with intel {SGX}. In *OSDI*.

[4] Maurice Bailleu, Jörg Thalheim, Pramod Bhatotia, Christof Fetzer, Michio Honda, and Kapil Vaswani. 2019. {SPEICHER}: Securing {LSM-based}{key-value} stores using shielded execution. In *FAST*.

[5] Johes Bater, Yongjoo Park, Xi He, Xiao Wang, and Jennie Rogers. 2020. Saqe: practical privacy-preserving approximate query processing for data federations. *PVLDB* (2020).

[6] Dan Bogdanov, Sven Laur, and Jan Willemson. 2008. Sharemind: A framework for fast privacy-preserving computations. In *ESORICS*.

[7] Dan Boneh, Eu-Jin Goh, and Kobbi Nissim. 2005. Evaluating 2-DNF formulas on ciphertexts. In *TCC*.

[8] Angela Bonifati, Wim Martens, and Thomas Timm. 2020. An analytical study of large SPARQL query logs. *VLDBJ* (2020).

[9] Ferdinand Brasser, Urs Müller, Alexandra Dmitrienko, Kari Kostiainen, Srdjan Capkun, and Ahmad-Reza Sadeghi. 2017. Software grand exposure:{SGX} cache attacks are practical. In *WOOT*.

[10] Jianneng Cao, Fang-Yu Rao, Mehmet Kuzu, Elisa Bertino, and Murat Kantarcioglu. 2013. Efficient tree pattern queries on encrypted xml documents. In *EDBT/ICDT*.

[11] Ning Cao, Zhenyu Yang, Cong Wang, Kui Ren, and Wenjing Lou. 2011. Privacy-preserving query over encrypted graph-structured data in cloud computing. In *ICDCS*.

[12] Zhao Chang, Lei Zou, and Feifei Li. 2016. Privacy preserving subgraph matching on large graphs in cloud. In *SIGMOD*.

[13] Stephen A Cook. 1971. The complexity of theorem-proving procedures. In *STOC*.

[14] Victor Costan and Srinivas Devadas. 2016. Intel SGX explained. *Cryptology ePrint Archive* (2016).

[15] Ningning Cui, Xiaochun Yang, Bin Wang, Jianxin Li, and Guoren Wang. 2020. SVkNN: Efficient secure and verifiable k-nearest neighbor query on the cloud platform. In *ICDE*.

[16] Grace Fan, Wenfei Fan, Yuanhao Li, Ping Lu, Chao Tian, and Jingren Zhou. 2020. Extending graph patterns with conditions. In *SIGMOD*.

[17] Zhe Fan, Byron Choi, Qian Chen, Jianliang Xu, Haibo Hu, and Sourav S. Bhowmick. 2015. Structure-preserving subgraph query services. *TKDE* (2015).

[18] Zhe Fan, Byron Choi, Jianliang Xu, and Sourav S. Bhowmick. 2015. Asymmetric structure-preserving subgraph queries for large graphs. In *ICDE*.

[19] Jiuru Gao, Jiajie Xu, Guanfeng Liu, Wei Chen, Hongzhi Yin, and Lei Zhao. 2018. A privacy-preserving framework for subgraph pattern matching in cloud. In *DASFAA*.

[20] Craig Gentry and Dan Boneh. 2009. *A fully homomorphic encryption scheme*.

[21] Oded Goldreich and Rafail Ostrovsky. 1996. Software protection and simulation on oblivious RAMs. *JACM* (1996).

[22] Johannes Götzfried, Moritz Eckert, Sebastian Schinzel, and Tilo Müller. 2017. Cache attacks on Intel SGX. In *EUROSEC*.

[23] Vincent Herbert, Bhaskar Biswas, and Caroline Fontaine. 2019. Design and implementation of low-depth pairing-based homomorphic encryption scheme. *JCEN* (2019).

[24] Haibo Hu, Jianliang Xu, Qian Chen, and Ziwei Yang. 2012. Authenticating location-based services without compromising location privacy. In *SIGMOD*.

[25] Kai Huang, Haibo Hu, Shuigeng Zhou, Jihong Guan, Qingqing Ye, and Xiaofang Zhou. 2021. Privacy and efficiency guaranteed social subgraph matching. *VLDBJ* (2021).

[26] Qin Jiang, Yong Qi, Saiyu Qi, Wenjia Zhao, and Youshui Lu. 2020. Pbsx: A practical private boolean search using Intel SGX. *Information Sciences* (2020).

[27] Hyunjoon Kim, Yunyoung Choi, Kunsoo Park, Xuemin Lin, Seok-Hee Hong, and Wook-Shin Han. 2021. Versatile equivalences: Speeding up subgraph query processing and subgraph matching. In *SIGMOD*.

[28] Hyunjoon Kim, Yunyoung Choi, Kunsoo Park, Xuemin Lin, Seok-Hee Hong, and Wook-Shin Han. 2022. Fast subgraph query processing and subgraph matching via static and dynamic equivalences. *VLDBJ* (2022).

[29] Hyeong-Il Kim, Hyeong-Jin Kim, and Jae-Woo Chang. 2019. A secure kNN query processing algorithm using homomorphic encryption on outsourced database. *DKE* (2019).

[30] Jinha Kim, Hyungyu Shin, Wook-Shin Han, Sungpack Hong, and Hassan Chafi. 2015. Taming subgraph isomorphism for RDF query processing. *PVLDB* (2015).

[31] Shangqi Lai, Xingliang Yuan, Shi-Feng Sun, Joseph K Liu, Yuhong Liu, and Dongxi Liu. 2019. GraphSE^2: An encrypted graph database for privacy-preserving social search. In *AsiaCCS*.

[32] Jinsoo Lee, Wook-Shin Han, Romans Kasperovics, and Jeong-Hoon Lee. 2012. An in-depth comparison of subgraph isomorphism algorithms in graph databases. *PVLDB* (2012).

[33] Xinyu Lei, Alex X Liu, Rui Li, and Guan-Hua Tu. 2019. SecEQP: A secure and efficient scheme for SkNN query problem over encrypted geodata on cloud. In *ICDE*.

[34] Jure Leskovec and Andrej Krevl. 2014. SNAP datasets: Stanford large network dataset collection. http://snap.stanford.edu/data.

[35] Yin Li, Dhrubajyoti Ghosh, Peeyush Gupta, Sharad Mehrotra, Nisha Panwar, and Shantanu Sharma. 2021. Prism: private verifiable set computation over multi-owner outsourced databases. In *SIGMOD*.

[36] Yehuda Lindell and Jonathan Katz. 2014. *Introduction to modern cryptography*.

[37] An Liu, Kai Zhengy, Lu Liz, Guanfeng Liu, Lei Zhao, and Xiaofang Zhou. 2015. Efficient secure similarity computation on encrypted trajectory data. In *ICDE*.

[38] Jinfei Liu, Juncheng Yang, Li Xiong, and Jian Pei. 2017. Secure skyline queries on cloud platform. In *ICDE*.

[39] Rongxing Lu, Xiaodong Lin, Zhiguo Shi, and Jun Shao. 2014. PLAM: A privacy-preserving framework for local-area mobile social networks. In *INFOCOM*.

[40] Shuai Ma, Yang Cao, Wenfei Fan, Jinpeng Huai, and Tianyu Wo. 2014. Strong simulation: Capturing topology in graph pattern matching. *TODS* (2014).

[41] Robin Milner. 1989. *Communication and concurrency*.

[42] Kartik Nayak, Xiao Shaun Wang, Stratis Ioannidis, Udi Weinsberg, Nina Taft, and Elaine Shi. 2015. GraphSC: Parallel secure computation made easy. In *S&P*.

[43] Miles Ohlrich, Carl Ebeling, Eka Ginting, and Lisa Sather. 1993. Subgemini: Identifying subcircuits using a fast subgraph isomorphism algorithm. In *DAC*.

[44] Pascal Paillier. 1999. Public-key cryptosystems based on composite degree residuosity classes. In *EUROCRYPT*.

[45] Claude E Shannon. 1949. Communication theory of secrecy systems. *Bell Syst. Tech. J.* (1949).

[46] Shweta Shinde, Zheng Leong Chua, Viswesh Narayanan, and Prateek Saxena. 2016. Preventing page faults from telling your secrets. In *AsiaCCS*.

[47] Yinglong Song, Huey Eng Chua, Sourav S Bhowmick, Byron Choi, and Shuigeng Zhou. 2018. BOOMER: Blending visual formulation and processing of p-homomorphic queries on large networks. In *SIGMOD*.

[48] Einat Sprinzak, Shmuel Sattath, and Hanah Margalit. 2003. How reliable are experimental protein–protein interaction data? *JMB* (2003).

[49] Yuanyuan Tian and Jignesh M. Patel. 2008. Tale: A tool for approximate large graph matching. In *ICDE*.

[50] Julian R Ullmann. 1976. An algorithm for subgraph isomorphism. *JACM* (1976).

[51] Sheng Wang, Yiran Li, Huorong Li, Feifei Li, Chengjin Tian, Le Su, Yanshan Zhang, Yubing Ma, Lie Yan, Yuanyuan Sun, et al. 2022. Operon: an encrypted database for ownership-preserving data management. *PVLDB* (2022).

[52] Songlei Wang, Yifeng Zheng, Xiaohua Jia, and Xun Yi. 2022. PeGraph: A system for privacy-preserving and efficient search over encrypted social graphs. *TIFS* (2022).

[53] Songlei Wang, Yifeng Zheng, Xiaohua Jia, and Xun Yi. 2022. Privacy-preserving analytics on decentralized social graphs: The case of eigendecomposition. *TKDE* (2022).

[54] Wai Kit Wong, David Wai-lok Cheung, Ben Kao, and Nikos Mamoulis. 2009. Secure knn computation on encrypted databases. In *SIGMOD*.

[55] Songrui Wu, Qi Li, Guoliang Li, Dong Yuan, Xingliang Yuan, and Cong Wang. 2019. Servedb: Secure, verifiable, and efficient range queries on outsourced database. In *ICDE*.

[56] Cheng Xu, Ce Zhang, Jianliang Xu, and Jian Pei. 2021. SlimChain: scaling blockchain transactions through off-chain storage and parallel processing. *PVLDB* (2021).

[57] Lyu Xu, Jiaxin Jiang, Byron Choi, Jianliang Xu, and Sourav S Bhowmick. 2021. Privacy preserving strong simulation queries on large graphs. In *ICDE*.

[58] Yuanzhong Xu, Weidong Cui, and Marcus Peinado. 2015. Controlled-channel attacks: Deterministic side channels for untrusted operating systems. In *S&P*.

[59] Xifeng Yan, Philip S Yu, and Jiawei Han. 2004. Graph indexing: a frequent structure-based approach. In *SIGMOD*.

[60] Bin Yao, Feifei Li, and Xiaokui Xiao. 2013. Secure nearest neighbor revisited. In *ICDE*.

[61] Can Zhang, Liehuang Zhu, Chang Xu, Kashif Sharif, Chuan Zhang, and Ximeng Liu. 2020. PGAS: Privacy-preserving graph encryption for accurate constrained shortest distance queries. *Information Sciences* (2020).

[62] Yandong Zheng, Rongxing Lu, Yunguo Guan, Songnian Zhang, Jun Shao, and Hui Zhu. 2022. Efficient and privacy-preserving similarity query with access control in eHealthcare. *TIFS* (2022).

[63] Wenchao Zhou, Yifan Cai, Yanqing Peng, Sheng Wang, Ke Ma, and Feifei Li. 2021. Veridb: An sgx-based verifiable database. In *SIGMOD*.

[64] Lei Zou, Lei Chen, and M Tamer Özsu. 2009. Distance-join: Pattern match query in a large graph database. *PVLDB* (2009).

A DEFINITIONS AND PROOFS

A.1 Definitions of *Strong Simulation*

DEFINITION 4. ***(Strong simulation (*ssim*) [57])*** *Given a connected query Q and a graph G, G is a* strong simulation *of Q, if G has a ball $B = G[v_s, d_Q]$, where $v_s \in V_G$, such that there exists a binary relation $S \subseteq V_Q \times V_B$, denoted by $\langle \cdot, \cdot \rangle$, satisfying the following conditions.*

(1) $\forall u \in V_Q$, $\exists v \in V_B$ such that $\langle u, v \rangle \in S$
(2) $\exists u \in V_Q$, such that $\langle u, v_s \rangle \in S$, and
(3) $\forall \langle u, v \rangle \in S$,
  (a) $L_Q(u) = L_B(v)$, i.e., $P(u, v) = 1$,
  (b) for all $u' \in V_Q$ where $M_Q(u, u') = 1$, there exists v' in V_B such that $M_B(v, v') = 1$ and $\langle u', v' \rangle \in S$, and
  (c) for all $u'' \in V_Q$ where $M_Q(u'', u) = 1$, there exists v'' in V_B such that $M_B(v'', v) = 1$ and $\langle u'', v'' \rangle \in S$. □

A.2 Proofs

In this appendix, we present the detailed proofs of the propositions of the paper.

PROPOSITION 1. *Given a query Q with diameter d_Q and label l ($l \in \Sigma_Q$), for any subgraph G_s of graph G, if G_s is a matching subgraph for Q under* hom*, there exists a vertex v in G such that i) $L_G(v) = l$, ii) G_s is a subgraph of $G[v, d_Q]$, and iii) $v \in G_s$.*

PROOF. W.l.o.g, assume vertex u in Q that satisfies $L_Q(u) = l$. Since G_s is a matching subgraph for Q under *hom* with a match function $\mathcal{H}$, there exists a vertex v in G_s that $\mathcal{H}(u) = v$ and hence, $L_{G_s}(v) = l$. For any vertex v' in G_s, we have $\text{dis}(v, v') \leq d_{G_s} \leq d_Q$ that $V_{G_s} \subseteq V_{G[v,d_Q]}$. Since $G[v, d_Q]$ (*resp.* G_s) is the induced subgraph of G based on the vertex set $V_{G[v,d_Q]}$ (*resp.* V_{G_s}), G_s is a subgraph of $G[v, d_Q]$. □

PROPOSITION 2. *Given a query Q, a label l ($l \in \Sigma_Q$), and a ball $B = G[w, d_Q]$ of a graph G, if there exists a subgraph B_s of B that B_s is a matching subgraph for Q under* hom *but $w \notin V_{B_s}$, there must exist a ball $B' = G[w', d_Q]$ of G that i) B_s is a subgraph of B', ii) $w' \in V_{B_s}$, and iii) $L_G(w') = l$.*

PROOF. Given a query Q and a label l ($l \in \Sigma_Q$), assume that the subgraph B_s of ball $B = G[w, d_Q]$ satisfies i) B_s is a matching subgraph for Q under *hom*, and ii) $w \notin V_{B_s}$. W.l.o.g, assume vertex u of Q satisfies that $L_Q(u) = l$. Since B_s is a matching subgraph for Q under *hom* with the match function $\mathcal{H}$, we have $\text{dis}\big(v, \mathcal{H}(u)\big) \leq d_{B_s} \leq d_Q$, $v \in V_{B_s}$. Therefore, ball $G[\mathcal{H}(u), d_Q]$ satisfies i) B_s is a subgraph of $G[\mathcal{H}(u), d_Q]$, ii) $\mathcal{H}(u) \in V_{B_s}$, and iii) $L_G\big(\mathcal{H}(u)\big) = l$. Prop. 2 holds. □

The proof of the query-obliviousness of Alg 1 in Sec. 3.1. Given a query Q and a ball B, Alg. 1 enumerates all CMMs of B by using only V_Q, Σ_Q and L_Q, where the pruning of redundant CMMs is independent of E_Q. Given any query Q' that i) $V_{Q'} = V_Q$, ii) $\Sigma_{Q'} = \Sigma_Q$, and iii) $L_{Q'} = L_Q$, Alg. 1 executes the same lines of code and returns the same set CM for Q'. Therefore, Alg. 1 is query-oblivious. □

The proof of the correctness of Alg. 2 in Sec. 3.2. Assume the CMM C represents a match function $\mathcal{H}_C$: $V_Q \to V_G$. According to CMM's definition (Sec. 3.1), $\mathcal{H}_C$ satisfies Condition (1) of Def. 1. Hence, matching violations can only be found for unsatisfaction on Condition (2) of Def. 1. That is, $\exists\, i, j \in [i, |V_Q|]$ such that $M_Q(i, j) = 1$ but $M_p(i, j) = 0$ since $M_p = C \cdot M_G \cdot C^{\mathrm{T}}$ is the projected adjacency matrix of G by C. To detect this unsatisfaction, we consider only two cases where $M_p(i, j) = 0$.

1. $\forall i, j$ that $M_p(i, j) = 0$, $M_Q(i, j) = 0$.
2. $\exists i, j$ that $M_p(i, j) = 0$, $M_Q(i, j) = 1$.

For Case 1, assume $\mathcal{H}_C$ does not satisfy Condition (2) of Def. 1. Then, there must exist vertices $u, v \in V_Q$ that $M_Q(u, v) = 1$ and $M_G(\mathcal{H}_C(u), \mathcal{H}_C(v)) = C(u) \cdot M_G \cdot C^{\mathrm{T}}(v) = M_p(u, v) = 0$, This is contradictory to Case 1 and hence, $\mathcal{H}_C$ satisfies Condition (2) of Def. 1 that $\mathcal{H}_C$ is a valid match function under *hom*. In this case, the encoding value 1 is multiplied into r in Line 6.

For Case 2, $\mathcal{H}_C$ cannot satisfy Condition (2) of Def. 1. That is, $\mathcal{H}_C$ is *not* a valid match function under *hom*. In this case, there exist i and j such that i) $M_p(i, j) = 0$, and ii) $M_Q(i, j)$'s encoding is $M_{Q_e}(i, j) = q$. Therefore, Line 6 aggregates (by multiplication) factor q into r.

In all, in Alg. 2, if C represents a valid match function under *hom*, only Case 1 exists that Line 7 returns r with an initial value 1. Otherwise, Case 2 also exists so that r is multiplied by a factor q by Line 6. □

The proof of the query-obliviousness of Alg. 2 in Sec. 3.2. Consider a graph G and any two distinct queries Q_1 and Q_2 that i) $V_{Q_1} = V_{Q_2}$, ii) $\Sigma_{Q_1} = \Sigma_{Q_2}$, and iii) $L_{Q_1} = L_{Q_2}$. Given a CMM for matching V_{Q_1} and V_{Q_2} to V_G, respectively, Lines 3-6 of Alg. 2 aggregate the encodings of elements located on the same positions in M_{Q_1} and M_{Q_2} into r, respectively. Therefore, the access pattern of encodings M_{Q_e} in Alg. 2 is independent of the query's edge set, *i.e.*, Alg. 2 is query-oblivious. □

PROPOSITION 3. *Consider a height h, a query Q, and a ball B with the center w. If there exists at least one $T^i_{v,h}$, $i \in$ {i, ..., x} where v is a vertex of Q but there does not exist $T^i_{w,h}$ s.t. $T^i_{v,h}$ and $T^i_{w,h}$ are isomorphic, then w cannot be matched to v under* sub-iso*,* hom *and* ssim*.*

PROOF. Prop. 3 is proved by contradiction. W.l.o.g, we prove Prop. 3 for the *hom* semantic, as the cases of *sub-iso* and *ssim* can be proved similarly. Given a match function $\mathcal{H}$ for matching V_Q to V_B under *hom*, we assume that the center w of B can be matched to a vertex v of Q. If there exists at least one $T^i_{v,h}$, $i \in$ {i, ..., x} but there does not exist $T^i_{w,h}$ such that $T^i_{v,h}$ and $T^i_{w,h}$ are isomorphic, then we cannot project a $T^i_{w,h}$ from B that is isomorphic to $T^i_{v,h}$, by using the vertices of B in $\{\mathcal{H}(u) \mid u \in \mathcal{V}\}$, where $\mathcal{V} = \{u \mid u \in V_{\mathrm{T}}, \mathbf{T}$ is a binary subtree of Q whose labels can be used to project the $T^i_{v,h}$ (according to Definition 3)$\}$. It contradicts with the definition of $\mathcal{H}$ such that the assumption is false and w cannot be matched to v. □

PROPOSITION 4. *Consider a query Q and a ball B with the center w. For any vertex u of Q that having the same label as w's label, if there exists one h-twiglet in Q starting from u but there does not exist such h-twiglet in B starting from w, w cannot be matched to u under* hom*,* sub-iso*, and* ssim *semantics.*

PROOF. Prop. 4 is proved by contradiction. W.l.o.g, we take *hom* as an example when the cases of *sub-iso* and *ssim* can be proved

in a similar way. Given a match function $\mathcal{H}$ of *hom* for matching V_Q to V_B. Assume that center w of B can be matched to vertex u of Q. If there exists one h-twiglet $t = [L_Q(u), L_Q(v_1), ..., [L_Q(v_{h-2}), L_Q(v_{h-1})]]$ in Q but there does not exist t in B starting from w, then there is a contradiction that the h-twiglet $[L_B(w), L_B(\mathcal{H}(v_1)), ..., [L_B(\mathcal{H}(v_{h-2})), L_B(\mathcal{H}(v_{h-1}))]]$ in B is identical to t. That is, t does not exist. Therefore, w cannot be matched u. □

B DETAILED PRIVACY ANALYSIS

In this section, we analyze the privacy of Prilo*, including 1) the privacy of encrypted messages, 2) the Prilo framework, 3) the BF pruning and the query-oblivious twiglet pruning techniques, and 4) the ball retrieval scheme. As introduced in Sec. 2.3, we assume both Dealer and Players are semi-honest [36], and Players do not collude with each other [35]. Moreover, we assume the collude-resistant model that Dealer and Player do not collude [15, 29, 37, 38].

B.1 Privacy Analysis of the Encrypted Messages

Prilo* uses the asymmetric encryption scheme CGBE [17] and *AES256* to encrypt the queries. The encrypted data of query Q include i) the encrypted encodings $M^E_{Q_e}$ of M_{Q_e} and the h-twiglet tables $\mathcal{T}$s that are encrypted by CGBE, and ii) the encrypted encodings of 2-label binary trees of Q's vertices that are encrypted by *AES256*. Then, we have the following proposition.

PROPOSITION 5. *Given a query Q, (i) the encrypted encodings $M^E_{Q_e}$ of Q's adjacency matrix, (ii) the twiglet tables $\mathcal{T}$s, and (iii) the encrypted encodings of 2-label binary trees of Q's vertices are preserved from* SP *against the attack model.*

PROOF. For the Player server, after receiving query Q from User, Players cannot break the ciphertexts in $M^E_{Q_e}$ and $\mathcal{T}$s since they are secure against *CPA* [17]. The encodings of 2-label binary trees of Q's vertices are encrypted by *AES256* and sent into Players' SGX's enclaves that Players cannot obtain the plaintexts of these encodings. Since Dealer i) does not have the private key of CGBE and *AES256*, and ii) cannot obtain these encrypted messages due to the assumption that Dealer and Players do not collude (Sec. 2.3), Prop. 5 holds. □

B.2 Privacy Analysis of the Prilo Framework

The Prilo framework has three steps, namely *candidate enumeration*, *query verification* and *query matching*. The analyses of their access pattern privacy are as follows.

• **Candidate enumeration.** As analyzed in Sec. 3.1, in the candidate enumeration algorithm (Alg. 1), all CMMs of a ball B are enumerated by using *only* V_Q, Σ_Q and L_Q of query Q, where the pruning of redundant CMMs is independent of E_Q. Given any other query Q' that i) $V_{Q'} = V_Q$, ii) $\Sigma_{Q'} = \Sigma_Q$, and iii) $L_{Q'} = L_Q$, Alg. 1 returns a CM of the same size for Q'. Therefore, Alg. 1 is query-oblivious.

• **Query verification.** As analyzed in Sec. 3.2, in the query verification algorithm (Alg. 2), the access pattern of encodings M_{Q_e} (or $M^E_{Q_e}$ after encrypted) is independent of query's edge set. Consider a graph G and any two distinct queries Q_1, Q_2 that i) $V_{Q_1} = V_{Q_2}$, ii) $\Sigma_{Q_1} = \Sigma_{Q_2}$, and iii) $L_{Q_1} = L_{Q_2}$. Given CMMs C_1 and C_2 for matching V_{Q_1} and V_{Q_2} (respectively) to V_G, Lines 3-6 of Alg. 2 aggregate the encodings of elements located at the same positions in M_{Q_1} and M_{Q_2}. Therefore, Alg. 2 is query-oblivious.

• **Query matching.** In this step, User decrypts the result set R from Player and then retrieves the target encrypted balls from Dealer. Although Dealer knows the specific balls retrieved by User, Dealer cannot infer any query edge information because Dealer has only the encrypted ball data (due to the assumption that Dealer and Players do not collude) without the secret key for the ball encryption. Hence, the query matching step is query-oblivious under our system and security model.

With the analyses above, the access pattern privacy is preserved by the Prilo framework. Regarding the query privacy, we make a few remarks. The inputs of Prilo in plaintext, V_Q, Σ_Q, L_Q and the ball B, have no relation to the query privacy. Moreover, d_Q does not lead to the query privacy leakage [18]. The ciphertexts used in Prilo on Players only are encrypted by CGBE and hence, are secure under *CPA* [17] so that the query privacy is preserved from Players. Therefore, we have the following proposition.

PROPOSITION 6. *The privacy target is preserved by the* Prilo *framework from* SP *against the attack model.*

B.3 Privacy Analysis of the Pruning Techniques

BF **pruning.** For the BF pruning in Sec. 4.1, we have the Prop. 7.

PROPOSITION 7. *The privacy target is preserved by the* BF *pruning from* SP *against the attack model.*

PROOF. On the User side, η (η is used to ensure the obliviousness and is set as a constant (256) in our experiments) encodings of 2-label binary trees of topologies vii-x in the query Q is computed without privacy leakage. On the Player side, the bloom filter of each candidate ball is constructed, which does not expose the query privacy since the construction process of bloom filters are independent of the query structure. The encodings of Q are encrypted and sent into SGX's enclave via a secure channel established between User and each Player's SGX while the bloom filters of candidate balls are transmitted into SGX's enclave directly on the Player side. As shown in Sec. 4.1.2, η encodings of Q are tested by the bloom filters in a query-oblivious manner inside the enclave, where the tested results are also aggregated into an integer in a query-oblivious manner. The integer is encrypted as c_{sgx} inside the enclave. Currently, SGX suffers from three types of leakages.

(1) The access pattern leakages through extensive observations and statistics in the untrusted memory access locations. Since the encodings of Q are tested by the bloom filters in a query-oblivious manner, this kind of access pattern is preserved.

(2) The access pattern leakages inside the enclave in a manner of page fault attacks [58]. Such attacks can be mitigated by a software-based defense solution [46]. Hence, we do not consider this kind of access leakages.

(3) The access pattern leakages using cache attacks [9, 22]. As our experimental settings show, the value of parameter m for the BF pruning (by Eqa. 1) is $25K$ that the size of each bloom filter is smaller than $4KB$ that can be addressed within one page. As the granularity of the attacks becomes finer, "the attackers become harder to get valid information" [26] from the memory access pattern.

With the analysis above, the access pattern privacy is preserved by the BF pruning from Players. Moreover, Q's encodings are obliviously tested by bloom filters inside SGX's enclave that the query privacy is also preserved from Players. Since Dealer is not involved in the BF pruning, Prop. 7 holds. □

Twiglet pruning. Let $\mathcal{G}(\mathcal{T}, i)$ $(resp.\ \mathcal{G}(r))$ be a function that returns 1 if SP can compute the corresponding plaintext of ciphertext c_{t_i} of h-twiglet t_i in $\mathcal{T}$ (*resp.* the output ciphertext r of Alg. 5) and returns 0, otherwise. Then, we analyze the probabilities of $\mathcal{G}(r) = 1$ and derive the following proposition.

PROPOSITION 8. *After running* `TwigletPrune`, $Pr[\mathcal{G}(r) = 1] \leq 1/2^n + \epsilon$, *where n is the number of ciphertexts c_ts aggregated into r in Line 10 of Alg. 5 and ϵ is a negligible value.*

PROOF. Given a query Q and a ball B with the center w, let $V_w = \{u \mid u \in V_Q$ and $L_Q(u) = L_B(w)\}$ and $W_w = \{h$-twiglet $t \mid t \in \mathcal{T}$ and t starting from vertex $u, u \in V_w\}$. For any h-twiglet $t_i \in \mathcal{T}$, t_i is encrypted by CGBE, which is secure against *CPA*. Hence, if attackers apply random guessing to attack t_i, then $Pr[\mathcal{G}(\mathcal{T}, i) = 1] \leq 1/2 + \epsilon'$, where ϵ' is a negligible value. For any two distinct h-twiglet t_i and t_js $\in \mathcal{T}$, we can know from the encoding and encryption scheme in Sec. 3 that their ciphertexts c_{t_i} and c_{t_j} are independent of each other, and $\mathcal{G}(\mathcal{T}, i) = 1$ and $\mathcal{G}(\mathcal{T}, j) = 1$ are therefore independent of each other. Then, we derive the following equation,

$$Pr[\mathcal{G}(r) = 1] = \prod_{t_i \in W_w} Pr[\mathcal{G}(\mathcal{T}, i) = 1] \leq \frac{1}{2^n} + \epsilon$$

where $n = |W_w|$ is the number of ciphertexts c_ts aggregated into r (Line 10 of Alg. 5) and ϵ is also a negligible value. Note that n is dependent of the structure of B but independent of the structure of Q. Therefore, Players cannot infer any information of c_{t_i} or r from the access pattern of Alg. 5. Since Dealer is not involved in the twiglet pruning, Prop. 8 holds. □

From Prop. 8, we can know that `TwigletPrune` preserves the query privacy from SP. With i) `TwigletPrune` is query-oblivious that preserves the access pattern privacy from Players, and ii) Dealer is not involved in the twiglet pruning, we derive Prop. 9.

PROPOSITION 9. *The privacy target is preserved by the twiglet pruning from* SP *against the attack model.*

B.4 Privacy Analysis of the Ball Retrieval Scheme

For the SSG scheme in Sec. 4.3, we have the following proposition.

PROPOSITION 10. *The privacy target is preserved by* SSG *from* SP *against the attack model.*

PROOF. With the assumption that Dealer and Player do not collude (Sec. 2.3), we analyze SSG's privacy preservation on Dealer and Player separately.

Privacy preservation from Dealer**.** From SSG, Dealer cannot know any information about the query privacy by using i) the decrypted *PM*s with ball identifiers sent from User, and ii) the computed ciphertext results sent from Players. This is because, as shown in Fig. 4, Dealer have only the encrypted ball data sent from DO but does not receive i) the secret key from DO to decrypt the ball data, and ii) the private key of CGBE from User to decrypt the ciphertext results. Although the access pattern for generating the sequences $\mathcal{S}_i$, $1 \leq i \leq k$ is not oblivious but related to the *PM*s, Dealer cannot infer any information about the query privacy from the access pattern by using the encrypted ball data. Therefore, the access pattern privacy is also preserved by SSG from Dealer and hence the privacy target is preserved by SSG from Dealer.

Privacy preservation from Player**s.** For each Player$_i$ $(1 \leq i \leq k)$, Player$_i$ receives from Dealer only a sequence $\mathcal{S}_i$ generated by SSG without knowing any information about the decrypted *PM*s used to generate $\mathcal{S}_i$. Therefore, the query privacy is preserved by SSG from Players as Players know only the ball data and the $\mathcal{S}_i$s without the plaintexts of the *PM*s when evaluating the balls. Next, we present that the access pattern privacy is also preserved by SSG from Players.

Given k Players, let $\mathcal{K}(i, j, \mathcal{S}_i)$ be a function that returns 1 if Player$_i$ $(1 \leq i \leq k)$ can determine whether the j^{th} ball in the sequence $\mathcal{S}_i$ spurious (negative or positive) and returns 0, otherwise. In the following, we show that attackers may only resort to random guessing to determine whether a candidate ball is spurious or not. First, we analyze the access pattern privacy preservation of RSG, which is used in the analysis for SSG.

(1) **The access pattern privacy is preserved by** RSG **from** Player**s.** We analyze the probabilities of $\mathcal{K}(i, j, \mathcal{S}_i) = 1$. Given a ball identifier set S with $|S| \cdot \theta$ positives, RSG randomly assigns the positives in S to sequences $\mathcal{S}_i$ for Player$_i$, $1 \leq i \leq k$. Assume $|S| \cdot \theta \cdot \beta_i$ positives are assigned to $\mathcal{S}_i$. According to the *Shannon's maxim* [45], Player$_i$ is assumed to know the sequence partition scheme without the value of θ and β_i, $1 \leq i \leq k$. Therefore, Player$_i$ cannot know whether a ball in $\mathcal{S}_i$ is negative. By applying random guessing, we have,

$$Pr[\mathcal{K}(i, j, \mathcal{S}_i) = 1] = \frac{1}{2} + \epsilon' \quad (2)$$

where ϵ' is a negligible value. Hence, the access pattern privacy is preserved by RSG from Players. In the following, we analyze the access pattern privacy preservation of SSG.

(2) **The access pattern privacy is preserved by** SSG **from** Player**s.** Let C_1 (*resp.* C_2) denote that SSG generates sequences $\mathcal{S}_i$, $1 \leq i \leq k$ according to the early case (*resp.* normal case) (Sec. 4.3). Given a ball identifier set S with $|S| \cdot \theta$ positives, the value of θ depends on the query structure and is unknown to Players. Therefore, when random guessing is used, the probability P_1 (*resp.* P_2) that Dealer generates sequences according to early case (*resp.* normal case) of SSG equals 1/2. Then, we analyze these two exhaustive cases below.

Early case $(\theta < 1/2)$**.** $\forall\ i \in [1, k]$ and $j \in [1, |S_i|]$,

– j is not larger than the SCP $(0 \leq j \leq \lceil 2|S| \cdot \theta / k \rceil)$**.** According to SSG, the numbers of positives and negatives before the SCP are the same. The balls before SCP are randomly permuted as shown in Fig. 9, Therefore, we have,

$$Pr[\mathcal{K}(i, j, \mathcal{S}_i) = 1 | C_1] = Pr[\mathcal{K}(i, j, \mathcal{S}_i) = 1] \cdot P_1 = \frac{1}{2} \cdot \frac{1}{2} < \frac{1}{2} + \epsilon \quad (3)$$

where ϵ is a negligible value.

– j is larger than the SCP $(\lceil 2|S| \cdot \theta / k \rceil < j \leq 2|S|/k)$**.** For the balls in $\mathcal{S}_i$ after the SCP, there are $\alpha = \lceil |S| \cdot \theta / k \rceil$ positives and $2|S|/k - 3\alpha$ negatives that are permuted randomly. Therefore, the probability that the j^{th} ball in the sequence $\mathcal{S}_i$ is positive (*resp.* negative) is $\alpha/(2|S|/k - 2\alpha)$ $(resp.\ (2|S|/k - 3\alpha)/(2|S|/k - 2\alpha))$. Note that θ is unknown to Players such that α is also unknown to Players. Therefore, by applying random guessing, we have,

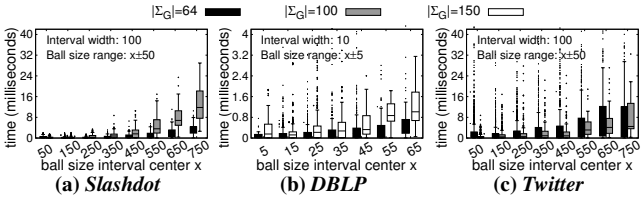

(a) *Slashdot* (b) *DBLP* (c) *Twitter*

Figure 19: Per-ball runtimes of $\texttt{BF}_{15}$ on three datasets

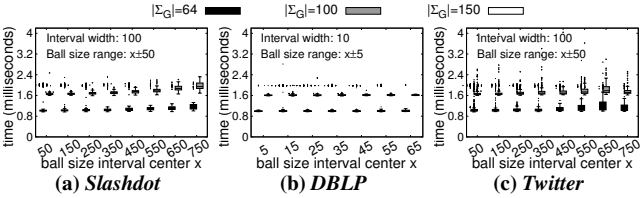

(a) *Slashdot* (b) *DBLP* (c) *Twitter*

Figure 20: Per-ball runtimes of $\texttt{Twiglet}_3$ on three datasets

$$Pr[\mathcal{K}(i,j,\mathcal{S}_i)=1|C_1] = Pr[\mathcal{K}(i,j,\mathcal{S}_i)=1]\cdot P_1 = (\frac{1}{2}+\epsilon')\cdot\frac{1}{2} < \frac{1}{2}+\epsilon \quad (4)$$

where ϵ is a negligible value.

Normal case ($\theta \geq 1/2$). SSG generates the subsequences $\mathcal{E}_i$ and $\mathcal{D}_i$ of sequence $\mathcal{S}_i$, $i \leq i \leq k$ by using RSG. According to Eqa. 2, we have,

$$Pr[\mathcal{K}(i,j,\mathcal{S}_i)=1|C_2] = Pr[\mathcal{K}(i,j,\mathcal{S}_i)=1]\cdot P_2 = (\frac{1}{2}+\epsilon')\cdot\frac{1}{2} \leq \frac{1}{2}+\epsilon \quad (5)$$

where ϵ is a negligible value.

Eqas. 3-5 show that the probability of successfully determining "$\mathcal{K}(i,j,\mathcal{S}_i)=1$" is low. The attackers can still rely on random guessing to attack the access pattern privacy. Since Players do not collude with each other, Player_i can learn nothing from the sequence $\mathcal{S}_i$. Therefore, the access pattern privacy is preserved by SSG from Players. As the query privacy is also preserved by SSG from Players, the privacy target is preserved by SSG from Players.

With the above analyses, Prop. 10 holds. □

In ⑨ of Fig. 4, although Dealer knows the identifiers of encrypted balls retrieved by User, Dealer can know nothing about the query privacy from the encrypted ball data. Then, by putting Props. 5, 6, 7, 9 and 10 together, we have Theorem. 1.

THEOREM 1. Prilo* *preserves the privacy target from* SP *against the attack model.*

C EXPERIMENTAL RESULTS

Overall runtime of $\texttt{BF}_{15}$. We investigate the BF pruning on the three datasets under the default setting. Fig. 19 shows $\texttt{BF}_{15}$'s runtime for each ball, including the runtimes of online bloom filter construction, data transmission into SGX's enclave, and oblivious testing on the bloom filters inside the enclave. We can see that the runtimes of $\texttt{BF}_{15}$ on all datasets increase as the ball sizes increase. This is because the complexity of subtrees' enumeration (Alg. 4) depends on the maximum degree of vertices of the ball, which often increases when the ball sizes increase. According to the statistics of candidate balls in Table 4, $\texttt{BF}_{15}$ may take hundreds of milliseconds for *hom* queries and few seconds for *ssim* queries.

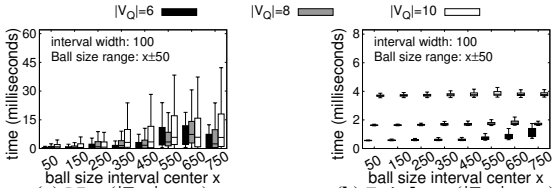

(a) $\texttt{BF}_{15}$ ($|\Sigma_G|$=100) (b) $\texttt{Twiglet}_3$ ($|\Sigma_G|$=100)

Figure 21: Per-ball runtimes by varying $|V_Q|$ on *Twitter*

Table 5: Characteristics of 20 *LDBC* business intelligence workloads

Query	$\|V\|$	$\|\Sigma\|$	d_Q	tested	Remarks
Q_1	1	1	0	×	single vertex
Q_2	3	2	2	×	path (undirected), always exists
Q_3	4	4	3	√	path (undirected)
Q_4	3	3	2	√	path (undirected)
Q_5	4	3	2	√	star (undirected)
Q_6	3	2	2	√	path (directed)
Q_7	4	2	2	×	contain negation
Q_8	2	2	1	×	pair, always exists
Q_9	3	3	2	√	path (directed)
Q_{10}	6	4	3	×	non-localized
Q_{11}	3	1	1	√	triangle (undirected)
Q_{12}	3	3	2	√	path (undirected)
Q_{13}	4	2	2	√	twig (directed)
Q_{14}	2	1	1	×	pair, always exists
Q_{15}	5	4	3	√	
Q_{16}	1	1	0	×	single vertex
Q_{17}	11	6	4	×	contain negation
Q_{18}	4	2	2	×	contain negation
Q_{19}	4	3	2	√	circle (undirected)
Q_{20}	2	1	1	×	non-localized

Overall runtime of $\texttt{Twiglet}_3$. Fig. 20 shows the per-ball runtimes of $\texttt{Twiglet}_3$. It can be seen that the runtimes of $\texttt{Twiglet}_3$ on *Slashdot* and *Twitter* increase slightly as the ball sizes increase. This is because $\texttt{Twiglet}_3$ involved *DFS* (Line 3 of Alg. 5) starting from the ball center to enumerate h-twiglets. For *DBLP*, $\texttt{Twiglet}_3$'s runtime is not sensitive to the ball size since *DBLP* is sparse that the ball sizes are not as large as the ones of *Slashdot* or *Twitter*, where the *DFS* visits few vertices. For the balls of graph G with a larger label set $|\Sigma_G|$, $\texttt{Twiglet}_3$ took more time to find a matching violation (Lines 6-11 of Alg. 5) due to more distinct labels of each vertex's neighbors. The relative performance of the techniques may vary with datasets. Compared to $\texttt{BF}_{15}$, $\texttt{Twiglet}_3$ took less time for *LPGM* queries on *Slashdot* and *Twitter*, but took more time when querying on the sparse dataset *DBLP*.

Runtimes of $\texttt{BF}_{15}$ and $\texttt{Twiglet}_3$ when varying $|V_Q|$. We varied the query sizes $|V_Q|$ = 6, 8, or 10 and denoted the queries as $Q_{|V_Q|}$. Fig. 21 shows the runtimes of $\texttt{BF}_{15}$, $\texttt{Twiglet}_3$ on *Twitter* for queries Q_6, Q_8 and Q_{10}. It can be observed from Fig. 21(a) that $\texttt{BF}_{15}$'s runtime increases slightly as $|V_Q|$ increases. This is because a larger $|V_Q|$ leads to a larger $|\Sigma_Q|$, which may increase the number of distinct labels of neighbors of each vertex of balls. From Fig. 21(b), we can see that the runtimes of $\texttt{Twiglet}_3$ increase as $|V_Q|$ increases since both a larger $|V_Q|$ and a larger $|\Sigma_Q|$ cost Alg. 5 more time.

***LDBC* business intelligence workloads**. To derive *LGPQ* queries from the *LDBC* business intelligence workloads, we made a few simplifications: For the 20 workload patterns, we omitted the value predicates (*e.g.*, *date* and *name*) of vertex label, reachability queries, negations, trivial structures (*e.g.*, single edge), and well-known relationships (e.g. "city" and "country"). Then, we obtain the structures of 10 out of 20 workloads. Table 5 shows some characteristics of these workloads.